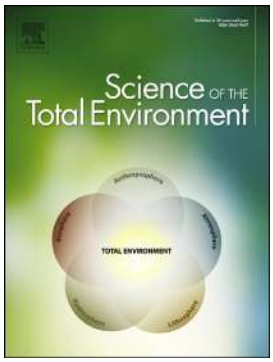

Assessing soil erosion risk at national scale in developing countries: The technical challenges, a proposed methodology, and a case history

Miluska A. Rosas, Ronald R. Gutierrez

PII: S0048-9697(19)35467-1

DOI: https://doi.org/10.1016/j.scitotenv.2019.135474

Reference: STOTEN 135474

To appear in: *Science of the Total Environment*

Received date: 23 July 2019

Revised date: 7 November 2019

Accepted date: 9 November 2019

Please cite this article as: M.A. Rosas and R.R. Gutierrez, Assessing soil erosion risk at national scale in developing countries: The technical challenges, a proposed methodology, and a case history, *Science of the Total Environment* (2019), https://doi.org/10.1016/j.scitotenv.2019.135474

Assessing soil erosion risk at national scale in developing countries: The technical challenges, a proposed methodology, and a case history

Miluska A. Rosas

Université catholique de Louvain, Louvain, Belgium
Pontificia Universidad Católica del Perú, Lima, Peru

Ronald R. Gutierrez

Universidad del Norte, Barranquilla, Colombia
Pontificia Universidad Católica del Perú, Lima, Peru

Abstract

Through an extensive bibliographic review, this contribution underlines the urgency and challenges to quantify soil erosion rates (ERs) in developing countries. It subsequently elaborates on the combined application of GIS-based RUSLE, generalized likelihood uncertainty estimation (GLUE) principles and sediment delivery ratio functions (SDR) to quantify ERs at country scale for these countries, as they commonly have limited measurements to that purpose. The methodology, termed RUSLE-GGS (RUSLE-GIS-GLUE-SDR) herein, comprises the following sequence: (1) construction of ER samples using RUSLE-GIS based on freely available local/global geoenvironmental observations and field relations, (2) construction of area-specific sediment yield samples utilizing SDR transfer functions, and (3) assessment of the most behavioral samples by means of bias analysis and cross validation. Its application to Peru allows obtaining 5-km resolution ER and potential erosion maps for the years 1990, 2000, and 2010. RUSLE-GGS is highly replicable and could potentially be used as an initial standard and systematic method to estimate ERs in developing countries through the active participation of local scientists. Thus, it potentially can contribute to improve the capacity building in such countries and set an initial frame to compare the evolution of soil erosion in their territories towards attaining Goal 15 of the UN 2030 Agenda for Sustainable Development.

Keywords: Soil erosion, uncertainty, RUSLE, land use change, developing countries

2010 MSC: 00-01, 99-00

*Corresponding author: rgutierrezll@uninorte.edu.co (Ronald R. Gutierrez)

1. Introduction

Soil erosion is a natural phenomenon mainly induced by site meteorological, topographical, geological, land cover conditions (e.g., soil disturbances related to deforestation, mining, agriculture, construction, urbanization, population growth, etc.), and underlying geomorphological processes such as hill slope erosion, mass movement, and channel erosion. Soil erosion will very likely be intensified by large scale anthropogenic controls such as global warming (Nearing et al., 2004; Lal et al., 2011). As a consequence, soil erosion represents a global societal concern because: (1) it often degrades soil and water resources and triggers economic losses in several countries all around the World (Ribaudo, 2009; Ayele et al., 2015), and (2) plays an important role in the global carbon cycle (Yang et al., 2003; Van Oost et al., 2007; Ito, 2007).

Some initiatives have been launched in recent years to improve World's social, economic, environmental conditions. The UN 2030 Agenda for Sustainable Development (United Nations, 2015) has set 17 goals for the year 2030 to that end. In specific, Goal 15 - life on land ("by 2030 governments need to protect, restore and promote sustainable use of terrestrial ecosystems, sustainably manage forests, combat desertification, and halt and reverse land degradation and halt biodiversity loss") is closely related to soil erosion. Lu et al. (2015) identified the following 5 priorities to accomplish these goals: (1) devising metrics so that the goals can be measurable, comparable and achievable: (2) establishing monitoring mechanisms to decide which values need to be tracked, and set up systems to acquire the data; (3) evaluating progress; (4) enhancing infrastructure, i.e. expanding Earth observation, ground-based monitoring and information processing capabilities; and (5) standardizing and verifying data, e.g. presenting the data as open access information.

Soil erosion rates (ERs) have been profusely estimated in developed countries through field, experimental and numerical modeling approaches, and at a wide range of spatio-temporal scales (Kirkby and Cox, 1995; Dedkov and Gusarov, 2006; Bellin et al., 2011; Morgan and Nearing, 2011; Cerdà et al., 2013). Conversely, a very limited number of such studies have been conducted in developing countries (Onyando et al., 2005; Shamshad et al., 2008; Labrière et al., 2015), even though there is a large suite of scientific evidence that (1) ERs are steadily increasing in their territories and likely reaching dramatics levels (Pimentel et al., 1995; Pham et al., 2001; Ananda and Herath, 2003; Boardman, 2006; Labrière et al., 2015; Borrelli et al., 2017), and (2) soil erosion is currently

one of the major environmental and geomorphic hazards exhibiting higher impacts in these countries (Alcantara-Ayala, 2002; Mondal et al., 2017). Thus, to attain Goal 15, the quantification of ERs in developing countries probably needs to be addressed with particular urgency.

Developing countries are mostly located in humid tropical regions (Sachs, 2001) and commonly face technical, financial, regulatory, and capacity-building challenges to improve the availability of: (1) spatio-temporal measurements and field relations to estimate ERs (Millward and Mersey, 1999; Labrière et al., 2015); and (2) soil erosion observations (e.g., ERs, frequency and extent of erosion, sediment yield) to calibrate or validate erosion models. In particular, sediment yield data is usually only available for large rivers, and, in many instances is insufficient in length, consistency, and continuity; and moreover, it is rarely publicly available (Labrière et al., 2015).

Several models to estimate ERs exist. They have been characterized as follows: (1) empirical or statistical models (e.g., SEDD, PSIAC) which are mainly based on the Revised Universal Soil Loss Equation, RUSLE; (2) conceptual models (e.g., SEDNET, SWAT), which commonly describe catchment processes without providing specific details of their interactions; and (3) physically based models (e.g., WEPP, PESERA, EUROSEM) which are based on the equations of conservation of mass and momentum for flow and the equations of conservation of mass for sediment (de Vente et al., 2013; Hajigholizadeh et al., 2018). The distinction between models is however diffuse for they couple modules from each of these categories (Ranzi et al., 2012; de Vente et al., 2013). Likewise, past research has highlighted the strong dependency of empirical, conceptual and physically based models on the availability of high resolution spatio-temporal input and calibration data, and the critical need of long and continuous simulations to reliably predict soil erosion (Merritt et al., 2003; Nearing, 2004; Ranzi et al., 2012; de Vente et al., 2013; Borrelli et al., 2017). Therefore, the selection of the most suitable model is subjected to the intended use and available data.

RUSLE was basically developed to estimate long-term average soil loss (i.e. gross erosion) and has been applied not only at small scales, but also at large scales, i.e. national, continental, and global scales (de Vente et al., 2005, 2008; Jetten and Maneta, 2011; Naipal et al., 2015; Panagos et al., 2015; Martin-Fernandez and Martinez-Nuñez, 2011). Typically, the main purpose of national scale estimations has been showing historical average erosion risk information to be used by policy-makers and territorial planning authorities, and to identify critical soil erosion prone areas that might need

institutional attention and/or require finer spatio-temporal assessment (Van der Knijff et al., 2000; Šúri et al., 2002; Terranova et al., 2009). Some of these estimates (Šúri et al., 2002; Terranova et al., 2009; Ranzi et al., 2012) were obtained by adopting Geographical Information System (GIS) techniques to treat data for the application to the RUSLE model.

In order to achieve Goal 15 of the UN 2030 Agenda for Sustainable Development, developing countries must firstly concentrate their efforts in the first and fifth priorities proposed by Lu et al. (2015). We posit that the studies to that end should be gradually conducted by local scientists to improve their capacity-building in these countries as well. Thus, it is reasonable to state that on the basis of Priority 1, there is a need to: (1) estimate soil erosion rates at both national scale and annual scale by following a standard method, (2) set a standard base line year for future comparison. The application of the RUSLE-GIS model based on publicly available local and satellite observations appears to be the most accessible mean to meet this necessity. That nevertheless demands generalizing detail in data and coping with the structural paucity of soil erosion measurements, which makes model validation challenging and imposes higher uncertainty into the model outputs.

Several studies have tackled RUSLE uncertainty. For instance, at global scale RUSLE-based ERs were validated using spatial extrapolation of plot experiments data from the NRI database for the USA and erosion estimates for Europe, and subsequently they were compared with global sediment yield observations from the World's major rivers (Pham et al., 2001; Van Oost et al., 2007; Ito, 2007; Naipal et al., 2015). Borrelli et al. (2017), meanwhile, used Markov Chain Monte Carlo approach. At catchment scale, RUSLE-based ERs have been validated using sediment delivery ratio (SDR) equations, in which SDR was used as a proxy parameter to estimate catchment sediment yield from gross erosion (Catari Yujra and Saurí i Pujol, 2010; Lee et al., 2014; Swarnkar et al., 2017). Likewise, Swarnkar et al. (2017) coupled Monte Carlo, RUSLE and SDR at catchment scale in India and obtained ER estimates with acceptable level of uncertainty.

In recent years Generalized Likelihood Uncertainty Estimation (GLUE) principles have been adopted to estimate the uncertainty of erosion models. For example de Vente et al. (2008); Jetten and Maneta (2011) coupled GLUE and SDR estimates to validate physically based erosion models at regional scale. GLUE considers that in field applications it is very difficult to specify a consistent model of the output errors due to our imperfect knowledge of the system and the associated uncertainty

of the input data, and by virtue of that, different parameter sets can produce acceptable results (Freer et al., 1996; Brazier et al., 2000, 2001; Aronica et al., 2002; Wei et al., 2008; Beven et al., 2008; Quinton et al., 2011). Far from the prevalent approach that parametrizes the RUSLE fundamental parameters and calibrate the outputs with local observations, an application of GLUE into RUSLE-based models would estimate the likelihood of a given set of models, parameters and variables. That would also agree with a body of evidence that suggests that model predictions that are produced through the random generation of parameter values can perform better than those produced by classical calibration (Brazier et al., 2000; Beven and Brazier, 2011).

This contribution aims to present a novel method termed RUSLE-GGS (RUSLE-GIS-GLUE-SDR) and has the following specific objectives: (1) describing the technical details of RUSLE-GGS, which unlike previous methodologies can potentially provide reliable ERs estimates at country scale to address the urgency to quantify the dynamics of soil erosion in developing countries in accordance to Goal 15 from the UN 2030 Agenda for Sustainable Development; and (2) elaborating on the application of RUSLE-GGS to Peru for the years 1990, 2000 and 2010.

2. Data and methods

2.1. Study area

2.1.1. Geoenvironmental conditions

Peru is located on the Neotropic ecoregion (Fig. 1-a). It occupies 1.29×10^6 km^2 and traditionally has been divided into three main natural regions (Fig. 1-b and 1-c), namely: coastal (western), andean (central), and amazonian (eastern), which occupy 12%, 28%, and 60% of the Peruvian territory, respectively. The main biomes in Peru (Fig. 1-c) are deserts and xeric shrublands (coastal region), montane grasslands and shrublands (andean region), and tropical and subtropical moist broadleaf forests (amazonian region) based on Olson et al. (2001).

According to the Köppen-Geiger climate classification scheme (Fig. 1-d): (1) the amazonian region mostly comprises types Af (tropical rainforest) in the Northern portion and Am (tropical monsoon) in the central and Southern portions; (2) the andean region mainly encompasses type Aw (tropical savannah) in the Northern portion and BSk (arid cold steppe) in the central and Southern portions; and (3) the coastal region mostly comprises type BWh (arid hot desert) in the Northern and central

portions and *BWk* (arid cold desert) in the Southern portion (Peel et al., 2007). Two global scale weather patterns control the climatic conditions of Peru, namely: (1) the tropical climate that affects 60.1% of South America (Peel et al., 2007); and (2) the occurrence of severe rainstorms when El Niño Southern Oscillation (ENSO) hits the arid coastal region (e.g., in 1972, 1983, 1987, 1998, 2015) causing dramatic changes in sediment fluxes at a multidecadal time scale (Quinn et al., 1987; Takahashi et al., 2011; Laraque et al., 2009). Global models also suggest that global warming could induce considerable precipitation variations in the Peruvian territory (Vuille et al., 2008).

2.1.2. Socio-economic conditions

From the 70's on Peruvian society has been transformed by the sustained growth of coastal urban centers as a result of massive migration of people from the andean region (Skeldon, 1977; Matos, 2012). Thus, in 2015, most of the Peruvian population lived in the coastal region (56.3%), followed by the andean region (29.7%), and the amazonian region (14%) (INEI, 2016). Peruvian economy chiefly relies on its natural resources such as mining in the andean region, and petroleum and gas in the amazonian region (Vuohelainen et al., 2012; OXFAM, 2014). Likewise, in 2012, the total cultivated land area was 0.07×10^6 km^2, which was distributed as follows: 46.3% in andean region, 30.1% in the amazonian region, and 23.7% in the coastal region (INEI, 2012). Peru is also steadily increasing its infrastructure portfolio.

2.1.3. Soil erosion features

Soil erosion in Peru is highly variable geographically and regarded as a very serious problem (World Bank, 2009). This high spatial variability is explained by particular topographic and climate controls such as: (1) the central Andes which is considered one of the global erosion hotspots on account of the convective storms it prompts in the dry highlands (Morera et al., 2013; Espinoza et al., 2012; Boardman, 2006; Borrelli et al., 2017); and (2) the Amazon rainforest that occupies a large portion of its territory. However, despite this critical condition there is not an specific erosion control regulatory framework in this country, and to the best of our knowledge, no quantitative study of soil erosion at national scale has been conducted for its territory. The last official map by INRENA (1996) solely presents qualitative information on the matter.

Peru has insufficient hydrometeorological observations to estimate sediment yield and ERs (Morera et al.,

Figure 1: (a) country location on terrestrial ecoregions; (b) main natural regions (limited by white dotted lines): coastal (western), andean (central), and amazonian (eastern); (c) Peru's main biomes after Olson et al. (2001); and (d) main climates after Peel et al. (2007): Af (tropical rainforest), Am (tropical monsoon), Aw (tropical savannah), BSh (arid hot steppe), BSk (arid cold steppe), BWh (arid hot desert), BWk (arid cold desert) Cfa (temperate, without dry season, hot Summer), Cfb (temperate, without dry season, warm Summer), and Cwb (temperate, dry Winter, warm Summer).

2013; Latrubesse and Restrepo, 2014). For instance, global estimates of suspended sediment fluxes by Peucker-Ehrenbrink (2009) were based on annual suspended sediment flux data from 599 rivers only covering 4.7% of rivers from western South America, yet no one represented the Peruvian

territory. Similarly, a small number of studies at field plot/hillslope scale (Alegre and Rao, 1996; Alegre and Cassel, 1996; Inbar and Llerena, 2000; Romero et al., 2007), and basin scale (Harden, 2006; Laraque et al., 2009; Tote et al., 2011; Morera et al., 2013; Pepin et al., 2013) were performed in Peru.

2.2. Data

Conducting temporal assessments of ERs at national scale in developing countries will possibly need setting a benchmark in the year 1990. That stems from resolution restrictions from satellite measurements and poor technical quality of information from local agencies prior to that year. Thus, for Peru such assessment is performed for the years 1990, 2000 and 2010 and is based on raw data described in Table 1, which can also be accessed from Rosas and Gutierrez (2017).

The raw data structure and data flow is depicted in Figure 1, which shows that the raw data was mainly used to obtain the fundamental parameters of RUSLE-GIS. The procedure to that end is detailed in the Supplementary Material.

Table 1: Input data used for the assessment of soil erosion in Peru for the years 1990, 2000 and 2010

	Description	Source	Resolution	Year	Reference
1	Global precipitation climatology project (GPCP)	NOAA	2.5°	1979-2009	Adler et al. (2003)
2	Tropical rainfall measuring mission (TRMM)	NASA	0.25°	1998-2010	Huffman et al. (2007)
3	Rainfall data	ANA[1]	Monthly	Varies	
4	Sand, silt and clay content maps	ISRIC - WSI[2]	1 km	2013	ISRIC (2013)
5	Organic carbon content map	ISRIC - WSI[2]	1 km	2013	ISRIC (2013)
6	ASTER digital elevation model	JSS[3] - NASA	30 m	2009-2011	METI and NASA (2011)
7	Global forest canopy height	ORNL-DAAC (NASA)	1 km	2011	ORNL-DAAC (2011)
8	Global land use/land cover images (15 classes)	USGS EROS	0.1°	1992-1993	Loveland et al. (2000)
9	The Global land cover facility (17 classes)	MODIS	0.25′	2001	Channan et al. (2011)
10	Global land cover share database (10 classes)	FAO	1km	2014	Latham et al. (2014)
11	Ecological Peruvian map (shapefiles, 106 classes)	ONERN[4]		1997	
12	Vegetative cover Peruvian map (shapefiles, 39 classes)	MINAM[5]		2010	

[1] Autoridad Nacional del Agua (Peru)
[2] World soil information
[3] Japan Space System
[4] Oficina Nacional de Evaluación de Recursos Naturales (Peru)
[5] Ministerio del Ambiente (Peru)

A set of stations (Table 2) were selected to obtain are-specific sediment yield (SSY) observations

from stream flow-sediment sampling stations and sediment reservoir surveys. They were chosen based on their free availability, and are spatially distributed to try to best represent Peru's meteorological and topographical characteristics. These stations encompass two watersheds running towards the Pacific Ocean (Jequetepeque, Chira, and Santa) and two watersheds running to Amazon tributaries (Urubamba, and Marañon). Additionally, we used the SSY estimate for the whole Eastern Peruvian Andes (average $1,113 \times 10^6$ t/y for the year 2005) by Latrubesse and Restrepo (2014), which was assumed to be valid for both the years 2000 and 2010, and later corroborated by our results.

Table 2: Area-specific sediment yield measurements ($SSY_{i,j,y}$) used in this study[1]

	Station	Station name	Station coordinates	Type[2]	Area (km^2)	Available data for	Res.[3]	y	Reference
1	Chira	Poechos	04°40'S, 80°30'W	RES	6,344	1976-2009	Y	1990, 2000, 2010	ANA (2010)
2	Jequetepeque	Gallito Ciego	07°06'S, 78°30'W	RES	3,317	1976-2009	M	1990, 2000, 2010	Technical report
3	Santa	Condorcerro	08°40'S, 78°16'W	SSS	10,415	1999-2009	M	2000, 2010	Morera et al. (2013)
4	Urubamba	Atalaya	10°44'S, 73°47'W	SSS	55,757	2004-2015	M	2010	Hybam[4]
5	Marañon	Borja	04°27'S, 77°27'W	SSS	42,561	2003-2016	M	2010	Hybam[4]
6	EPA[5]			REG	298,530	2004-2006	Y	2000	Latrubesse and Restrepo (2014)

[1] All the data is presented in Rosas and Gutierrez (2017)
[2] RES=reservoir, SSS=streamflow sediment sampling station, REG=region
[3] Resolution: Y=yearly, M=monthly
[4] Hybam website: `http://www.ore-hybam.org/`
[5] EPA=Eastern Peruvian Andes

2.3. Methods

RUSLE-GGS is aimed to assess the uncertainty in using the RUSLE-GIS model to estimate soil ERs at national scales in developing countries. It tackles such uncertainty by using the GLUE method, which is adapted in this study in the following sequence:

(i) *Construction of ER samples*: a set of RUSLE-GIS samples are built from realizations of the fundamental model parameters (see the Supplementary Material on RUSLE-GIS). These realizations are constituted by available local and global geoenvironmental data and field relations.

(ii) *Construction of area specific sediment yield samples (SSY*)*: SDR equations are utilized as transfer functions to create SSY^* samples from ER samples.

(iii) *Assessment of the most behavioral ER samples*: past research standards are applied to define the likelihood bound of SSY*. Subsequently, behavioral SSY* samples are identified by performing cross validation of the ER parameters transferability to select the behavioral ER sample for a given year. Additionally, behavioral ER samples are compared with results from global models.

The main building blocks of the application of RUSLE-GIS to Peru are displayed in Fig. 2 and are fully described as follows. The reader can access to all the information to build ER and SSY^* samples from Rosas and Gutierrez (2017).

Figure 2: Flow diagram of the main building blocks of RUSLE-GGS. See the Supplementary Material for technical details on RUSLE-GIS.

2.3.1. Construction of RUSLE-GIS-GLUE based ER samples

A matrix $\left\{E_y^{[1]}, E_y^{[2]}, \ldots, E_y^{[24]}\right\}$ of 24 $E_y^{[k]}$ ER samples using Eq. A.1 were built for each year of study y, where $y \in \{1990, 2000, 2010\}$. Each $E_y^{[k]}$ was based on the following N realizations of the five fundamental parameters of RUSLE which are presented in detail in the supporting information by Rosas and Gutierrez (2017):

(i) Six realizations ($N = 6$) of the rainfall erosivity factor obtained by using satellite precipitation data ($\left\{R_y^{[1]}, \ldots, R_y^{[3]}\right\}$) and ground precipitation measurements ($\left\{R_y^{[4]}, \ldots, R_y^{[6]}\right\}$) as input parameters for Eqs. A.2a-A.2d. The equation by (Renard and Freimund, 1994), which is only applicable to regions exhibiting low precipitation rates, was used solely in regions having less than 200 mm of annual precipitation, i.e., mainly in the coastal region that comprises class $Ea23$ and $Aa22$ arid land areas.

(ii) One realization ($N = 1$) for the soil erodibility factor (K) defined by Eq. A.3 which remains static for each year y.

(iii) Two realizations ($N = 2$) for the cover and management factor based on the data source from which were obtained, namely: $C_y^{[1]}$ from global data, and $C_y^{[2]}$ from data published by local agencies.

(iv) Two realizations ($N = 2$) of the slope length/steepness (LS) factor, namely, $LS^{[1]}$ from Eqs. A.4a-A.4d, and $LS^{[2]}$ based on the LS-TOOL output, which remain static for each year y.

(v) One realization ($N = 1$) for the support practice factor P (Eq. A.5).

2.3.2. Construction of area-specific sediment yield samples (SSY)*

Sediment production can be described by: (1) SY and area-specific sediment yield (SSY) measured at either streamflow-sediment sampling stations or sediment reservoir surveys; and (2) sediment delivery ratio (SDR) representing the fraction of soil erosion supply from the catchment to the streams, i.e. the ratio between SY and ER (Alatorre et al., 2010; Vigiak et al., 2012). Thus, by using bulk area-specific ER ($\bar{E}_y^{[k]}$ in $t/h/y$ in Eq. 1) from j specific locations and a set of SDR transfer functions (Table 3), proxy area-specific sediment yield samples ($SSY_{i,j,y}^{*}$ in Eq. 1) were

Table 3: SDR transfer functions utilized to obtain SSY* samples

Equation	Parameters description	Area (km^2)	Source
$SDR_1 = 0.627 \times (SLP)^{0.403}$	SLP: slope of the main stream channel in %	0.5-18	Williams and Berndt (1972)
$SDR_2 = 1.817 \times A^{-0.132}$	A: catchment area in km^2	6.6-800	Sharda and Ojasvi (2016)
$SDR_3 = exp\{1.7935 - 0.14191 \times \log A\}$	A: catchment area in km^2	1-262	Renfro (1975)
$SDR_4 = 0.42 \times A^{-0.125}$	A: catchment area in mi^2	1-500	Vanoni (1975)
$SDR_5 = 0.51 \times A^{-0.110}$	A: catchment area in mi^2	0.5-150	USDA-NRCS (1979)
$SDR_6 = 1.366 \times 10^{-11} \times A^{-0.00998} \times (ZL)^{0.3629} \times (CN)^{5.444}$	A: catchment area in km^2 ZL: relief-length ratio in m/km CN: long-term average US Soil Conservation Service curve number that is used to estimate runoff	200	Williams (1977)

obtained.

$$SSY^*_{i,j,y} = SDR_i \times \bar{E}^{[k]}_y; \text{ for } i = 1, 2, \ldots, j \tag{1}$$

SDR_i is a dimensionless parameter expressed in decimal form and $SSY^*_{i,j,y}$ is expressed in $m^3/h/y$ after assuming an average sediment specific weight of 1.2 t/m^3 (Montgomery, 2007; Ito, 2007).

2.3.3. Assessment of the most behavioral ER samples

GLUE requires determining a likelihood measure to assess the goodness of fit between SSY* and SSY observations (Table 2). However, since in most of environmental modeling it is difficult to define a likelihood measure to that purpose, the choice of likelihood based on GLUE is in general subjective, the only formal requirement is that it should be zero for all non-behavioral outputs (Brazier et al., 2000). In this study, two likelihood functions were employed: the bias and the Nash-Sutcliffe index. Past GLUE applications in soil erosion and hydrologic modeling (Kim and Gilley, 2008; Houska et al., 2014) have used the bias function (Eq. 2) to quantify the model tendency to over or under estimate the measurements. Other soil erosion studies (Bingner et al., 1989; Hui et al., 2010) have accepted SY rates results differing less than 20% from SY measurements. RUSLE-GGS hence assumes an a priori bias of ±20% respect to SSY measurements (dotted horizontal lines in Figure 3).

$$Bias = \frac{SSY - SSY^*}{SSY} \times 100 \tag{2}$$

After selecting the scenarios falling inside the bias acceptable bounds, a full cross validation for all the stations was performed. It basically implied testing the parameter settings of a behavioral sample $E_y^{[k]}$ on another site and vice versa. The Nash-Sutcliffe index (NSE in Eq. 3) was subsequently used to quantify the model's sensitivity to outliers. In Eq. 3 $\overline{SSY}$ represents the mean SSY from j observations for a given year y. NSE=1 when the model predicts the observations perfectly and NSE=0 when the model has the same goodness of fit as the observations average (de Vente et al., 2013). Samples having $NSE < 0$ imply that the cross validation produces more variation than the observations (Betrie et al., 2011; Haregeweyn et al., 2013; Houska et al., 2014).

$$NSE = 1 - \frac{\sum_{m=1}^{j}(SSY_m - SSY_m^*)^2}{\sum_{m=1}^{j}(SSY_m - \overline{SSY})^2} \tag{3}$$

A second-stage assessment was performed by comparing RUSLE-GGS outputs with those from global erosion models by Kirkby and Cox (1995); Van Oost et al. (2007); Doetterl et al. (2012); Naipal et al. (2015). The assessment mainly consisted on comparing the orders of magnitude of bulk erosion rates and potential soil erosion (PE in Eq. 4 expressed in $t/h/y$) at the coastal ($176,117\ km^2$), andean ($361,929\ km^2$), and amazonian ($751,075\ km^2$) regions based on the regional limits displayed in Fig. 1-b. PE is defined as the product of the R, K, L, and S RUSLE factors. PE maps reflect the soil vulnerability to erosion when it does not have any vegetative cover and any erosion control practice is implemented, and thereby provides information on the most critical scenario for soil erosion hazard (Šúri et al., 2002).

$$PE = R \times K \times L \times S \tag{4}$$

3. Results

3.1. RUSLE-GGS efficiency

Equations A.1 through A.5 were used to build 24 ER samples ($\left\{E_y^{[1]}, \ldots, E_y^{[24]}\right\}$), and subsequently, by using 6 SDR transfer functions (Table 3), 144 area-specific sediment yield samples (SSY^*) were obtained for each year $y \in \{1990, 2000, 2010\}$, and for each station in Table 2. Thus, this study is based on 1,728 SSY^* samples whose likelihood were evaluated by using the Bias func-

Figure 3: Assessment of the behavioral SSY^* samples for the years 1990, 2000 and 2010. Black dotted lines represent the Bias function upper and lower 20% limits. Red circles depict non-behavioral samples, and blue filled squares depict behavioral samples laying inside the Bias function acceptable area. Black triangular marks represent the behavioral samples having $NSE > 0$.

tion (Eq. 2) and the Nash-Sutcliffe index (Eq. 3).

A custom computer program was built to analyze the spatio-temporal likelihood distributions of the SSY^* samples. Figure 3 shows the results from both the streams flowing to the Pacific Ocean (Stations 1, 2, and 3) and to the Amazon River (Stations 4, 5, and 6). In Fig. 3, the bias bounds

of $\pm 20\%$ are represented by horizontal dotted lines which allowed for identifying 131 out of 1,728 behavioral SSY^* samples. The assessment of the behavioral SSY^* samples through cross-validation indicates that 6 out of 131 present $NSE > 0$.

The behavioral samples are predominantly obtained by using the SDR_1 transfer function (Fig. 4-a), rainfall erosivity factor $R^{[1]}$ (Eq. A.2a using satellite precipitation input data), cover and management factor $C^{[1]}$ (based on global data) and slope length/steepness factor $LS^{[2]}$ (LS-TOOL output), which together constitute $E^{[13]}$ (Fig. 4-b). These samples are spatially distributed as follows: 51 correspond to Pacific streams (Fig. 4-c-d) and 80 to Amazonian streams (Fig. 4-e-f). They are temporally distributed in this fashion: 20 (1990), 65 (2000), and 46 (2010).

The accuracy of RUSLE-GGS outputs is described herein in terms of the average of the behavioral samples ($\overline{SSY^*}$), which as anticipated, exhibits strong spatio-temporal variability. In 1990, $\overline{SSY^*} = 0.37 \times 10^6\ m^3/h/y$ at Gallito Ciego station (Jequetepeque basin), and $\overline{SYY^*} = 3.35 \times 10^6\ m^3/h/y$ at Poechos station (Chira basin). Similarly, for the year 2000, $\overline{SSY^*}$ rates of 2.96 and $28.3 \times 10^6\ m^3/h/y$ were obtained at these stations. Interestingly enough, no behavioral sample exists for the Condorcerro gauging station (Santa basin).

In the whole Eastern Peruvian Andes we estimated an average SY of $984 \times 10^6\ t/y$, which lays very close to that obtained in that study ($1,113 \times 10^6\ t/y$). RUSLE-GGS exhibits a low performance for the year 2000. It nevertheless best performs in 2010, in which $\overline{SYY^*}$ estimates of 4.7, 3.1, 3.7, 99.4, and $219.7 \times 10^6\ m^3/h/y$ were obtained for the Condorcerro, Gallito Ciego, Poechos, Borja, and Atalaya stations, respectively (Fig. 5-i). Our results also indicate that SSY^* rates in Santa, Chira, Urubamba, Marañon, and Jequetepeque rivers are proportional to the basin area.

After assessing the behavioral samples, PE maps (Fig. 5a-c) and ER maps (Fig. 5d-f) were developed for the years 1990, 2000, and 2010. They show that RUSLE-GGS provides estimates that have the same order of magnitude as those from global soil erosion models for the years 1990 and 2000, and for the coastal and amazonian regions (Fig. 1-b), although it is not always the case for the andean region.

Figure 4: Probability of: (a) SDR transfer functions, (b) ER samples based on the SSY^* behavioral samples, (c-d) SDR transfer functions and ER samples for streams flowing to Eastern Andes, and Western Andes (e-f). From 1990 to 2010, the most probable ER sample is $E^{[13]}$ which is constituted by $R^{[1]}$, $C^{[1]}$, $LS^{[2]}$.

3.2. Spatio-temporal evolution of ERs in Peru

For the period 1990-2010, ER maps evince that the mean highest ERs ($> 50\ t/h/y$) are found in the andean (31%) and coastal (11%) regions. Conversely, for the same period, low ERs ($< 10\ t/h/y$) persistently covers $\sim 60\%$ of the amazonian region. As expected, the andean region presents the highest PE ($> 500\ t/h/y$), which covers $\sim 39\%$ of its territory.

A spatio-temporal analysis of ERs emphasizes that moderate rates ($10 - 50\ t/h/y$) have notably increased in the the western Peruvian Andes and the coastal region for the periods 1990-2000 (Fig. 5.d) and 2000-2010 (Fig. 5.e).

The average national ER shows the following evolution: $\sim 24\ t/h/y$ (1990), $\sim 12\ t/h/y$ (2000) and $\sim 33\ t/h/y$ (2010). For the period 1990-2000 the highest ERs in the country increased 3% in average; similarly, for 2000-2010 it increased 10%. The highest increase is observed in the andean region, as follows: 10% (1990-2000) and 30% (2000-2010).

As shown in Figure 6, for the year 2010, Moquegua and Apurimac provinces (southern Peru, Fig. 5-f), which are mostly located in the andean region, feature the highest proportion of their territories with severe erosion.

Figure 5: RUSLE-GGS output for Peru at 5-km resolution. (a)-(c) PE rates maps for 1990, 2000 and 2010, respectively. (d)-(f) ER maps for the same years. (g) ER gradients maps for period 1990-2000 and 2000-2010 (h). (i) locations of the SSY gauging stations and the limits of the Eastern Peruvian Andes region after Latrubesse and Restrepo (2014).

4. Discussion

4.1. RUSLE-GGS, the proposed methodology

The critical affectation of many developing countries by soil erosion has been reported in several studies (Pimentel et al., 1995; Pham et al., 2001; Alcantara-Ayala, 2002; Ananda and Herath, 2003; Boardman, 2006; Labrière et al., 2015; Mondal et al., 2017; Borrelli et al., 2017). As described in Section 2.1, Peru, an upper-middle-income economy, epitomizes such situation. It is therefore reasonable arguing that it might be much worse in poorer countries.

Soil erosion studies require quantifying uncertainties associated to the complexity of the physical pro-

cesses and the scarcity of accurate field observations for calibration (Cea et al., 2016). Even though developed countries have considerable SY and ER field datasets, still several researchers believe that they are not long enough to apply and calibrate sophisticated soil erosion models (Ferro and Porto, 2000; Nearing, 2004). As highlighted in this contribution, developing countries feature insufficient input data and restricted observations to calibrate erosion models. For example, water discharge and SY are poorly characterized at the western South America (Peucker-Ehrenbrink, 2009), possibly because collecting SY measurements is expensive (Hudson, 1993; McCool and Busacca, 1998; Onyando et al., 2005). As a consequence, sophisticated models only can be applied to a very limited number of watersheds.

Empirical models such as RUSLE are relatively simple, robust in structure and thereby, have been widely used in the assessment of soil erosion under scarcity of field data, and when integrated with GIS on grid-cell basis, it allows for analyzing spatially distributed soil erosion potential effectively (Terranova et al., 2009; Ganasri and Ramesh, 2016; Singh and Panda, 2017). The accuracy of RUSLE also results in some cases is approximately similar as that for the WEPP model which nevertheless needs finer resolution data (Nearing, 2004). RUSLE does not quantify sediment yield at the outlet of the watershed; nonetheless, a reliable assessment of SDR can be performed by using observed sediment yield at a watershed section or reservoir from RUSLE outputs. That is the case reported by Lee et al. (2014), who obtained relative errors between 6.4% and 13.5% for the Gyeongan River (561 km^2), Korea.

As shown in this study, in the context of developing countries, and under the urgent challenge of estimating erosion rates at country scales, the combined application of RUSLE-GIS, GLUE, and SDR transfer functions (RUSLE-GGS) can provide estimates with quantitatively-known uncertainties.

Most studies at large scales rarely have used spatial output for verification (Jetten and Maneta, 2011). Our results are yet quantitatively assessed by following the GLUE methodology and SSY field data. GLUE and Bayesian approaches have been criticized for having limitations in quantifying model output uncertainty (Beven et al., 2008), recent studies however suggest that even imprecise historical data can markedly decrease a model uncertainty (Salinas et al., 2016). Therefore, we believe that although ER field data and observations of RUSLE factors are limited/nonexistent in developing countries, it is highly probable finding even "fuzzy" data from sediment loads of rivers

and siltation of dams and reservoirs that could improve the efficiency of RUSLE-GGS. That being so, it is reasonable stating that that RUSLE-GGS can potentially be applied in most developing countries, yet its results should be regarded as preliminary. This stems from the fact that RUSLE estimates are regarded as broad scale erosion surveys for assessing ER spatio-temporal evolution, but are not useful as storm-response design tools (Nearing, 2004).

Recently, some members of the scientific and intergovernmental communities have underscored the need to adopt open-science data practices, and promote the use of steadily increasing Earth observations (Showstack, 2015). We believe that RUSLE-GGS could contribute to these ends if it is adopted as an initial standard frame to quantify ERs for developing countries. These ERs could subsequently become freely accessible to guide the decisions and actions to efficiently manage soil resources in such countries, this information could also be assimilated into physically-based models to improve the scientific understanding of the mechanisms that describe soil erosion in the tropics. Likewise, RUSLE-GGS can provide information to implement metrics of sediment connectivity (e.g., Heckmann et al., 2018; Grauso et al., 2018) to quantify the vulnerability to the offsite effect of soil erosion. For these reasons, we believe that a systematic and standardized application of RUSLE-GGS may contribute to accomplish with the soil-erosion-related Goal 15 of the UN 2030 Agenda for Sustainable Development which requires using: (1) geographical information systems to host and share data from the observing networks; and (2) simulation and decision-making tools to support sustainability planning, management and enforcement (Lu et al., 2015).

4.2. Application of RUSLE-GGS to Peru

The application of RUSLE-GGS over Peru was performed using input data consisting on satellite measurements and, to a lesser extent, observations provided by local public agencies. However, all the aforementioned information does not allow to discern which of these controls are more predominant in inducing such evolution. That certainly deserves further research.

Apparently, SRTM performs better than other digital elevation models in improving the efficiency of RUSLE (Mondal et al., 2017). Such evidence was not evaluated in this contribution, yet two realizations of the slope length/steepness factor (LS) were built from the ASTER DEM. RUSLE typically shows high sensitivity to the rainfall erosivity (R) and cover and management (C) factors

Figure 6: Territorial categorical distribution of ERs in Peru for the year 2010.

(Jetten and Maneta, 2011). When the latter is calculated on an annual basis, apparently the main source of uncertainty is the temporal variability of precipitation at wider spatial scales (Catari et al., 2011). Even though six realizations of the R factor were obtained for this study, we hypothesize that the efficiency of RUSLE-GGS could be improved if R is estimated from the direct analysis of hourly/sub-hourly precipitation measurements. That would require quantifying the average annual summation of individual storm erosivities (Nearing, 2004). Unfortunately, only monthly precipitation data was freely available for our study.

Peru exhibits an insufficient density of SSY gauging stations (Latrubesse and Restrepo, 2014), even though it is an upper-middle-income-economy. For instance, Syvitski and Milliman (2007) used two global datasets containing information from large and small rivers. Even so, none of them included Peruvian rivers draining to the Pacific Ocean because such information was not available.

Our results show a positive correlation between SSY^* and catchment area, although past studies indicate that it may increase or decrease as a function of drainage area (Cerdà et al., 2013). The identification of behavioral SSY^* samples were based on six watersheds, which represent the data solely available from technical reports, past studies, and reliable institutions (e.g. Hybam) for Peru. A relaxed threshold for the Nash-Sutcliffe index was assumed (i.e., $NSE > 0$), as formulated by

Houska et al. (2014). No one of the behavioral samples belongs to the year 2000, which suggests that such year is an outlier. Most behavioral samples were obtained per unit reservoir than that per unit stream flow sediment sampling station. For instance, no behavioral sample was obtained for the Cordorcerro gauging station. This might stem from the fact that (1) generally small rivers are more responsive to episodic events (Syvitski and Milliman, 2007), or (2) reservoir surveys commonly provide more reliable SSY measurements than gauging stations (de Vente et al., 2013).

RUSLE-GGS' performance in somewhat low in the year 2000, probably triggered by the 1998 ENSO event as ENSO plays an important role in the erosion processes in the Peruvian northern coastal area (Quinn et al., 1987). However, the model performance markedly improves in the year 2010, may be because there were more freely accessible observations for that year.

The model outputs have the same order of magnitude as some global models. For instance, the ER 1990 map (Fig. 5.d) shows that in the amazonian region, the mean ER was $\sim 2\ t/h/y$, similar to that obtained by Pham et al. (2001) $(0 - 10\ t/h/y)$. Our result for the coastal region $(\sim 85\ t/h/y)$ is also comparable to that by Pham et al. (2001) $(10 - 50\ t/h/y)$, it is however slightly higher in areas having poor density of rainfall ground stations (see the Supplementary Material). For the year 2000, the RUSLE-GGS outputs differ from the global model by Doetterl et al. (2012), though it has same order of magnitude. Our results for the the year 2010 can only be comparable with the continental ER obtained by Doetterl et al. (2012) $(12 - 18\ t/h/y)$ and that for the average country ER $(\sim 33\ t/h/y)$. Our ER estimates for the andean region are: 39 (1990), 32 (2000), 101 $t/h/y$ (2010) which are in the ER range $(0.3 - 151\ t/h/y)$ obtained by Molina et al. (2008) for a central Andean region.

Over all, our results exhibit the same pattern observed in most of erosion models: they tend to overestimate erosion rates during years when little erosion occurs (e.g. when no ENSO events occur) and underestimates it during years when erosion is significant (e.g. during the strong 1998 ENSO) as reported by Beven and Brazier (2011). Despite these restrictions RUSLE-GGS allowed for obtaining both ER and PE maps for Peru which, to the best of our knowledge, would be the first publicly available quantitative maps.

The aforementioned maps suggest that moderate ERs in Peru are rapidly increasing in the coastal and andean regions. This pattern is similar to the global trend reported by Pham et al. (2001);

Van Oost et al. (2007); Ramankutty et al. (2008); Doetterl et al. (2012). The highest ERs are also located in these regions. This may stem from the fact that the andean region presents steep hills and periods of high rainfall that play an essential role in the production of SY and soil erosion (Michaelides and Martin, 2012). It is unclear nevertheless whether soil erosion is predominantly determined by natural or anthropogenic controls. The same conclusion was draw in a catchment-scale study by (Vanacker et al., 2007) in an andean area from Ecuador.

Highest ERs in the coastal region are possibly controlled by variations in the C factor due to land development as the population grew from 54.6% to 63.4% of the country's population for the period 2007-2014 (Paulet and Amat, 1999; World Bank, 2015; MINAR, 2015; INEI, 2014). Since this region is seismically highly active, soil erosion and landslides may also be positively correlated with earthquakes as past research (Scheidegger, 1992; Scheidegger and Ai, 1986) suggests.

The amazonian region exhibits the lower ERs in Peru and the lowest increase on it. This corroborated our assumption that the ER in the Eastern Peruvian Andes by Latrubesse and Restrepo (2014) was somewhat invariant for both the years 2000 and 2010.

The average national ER exhibits an increasing trend, similarly to that reported by Borrelli et al. (2017), that might persist due to the steady growth of the Peruvian population and the increase of the extension of areas granted to the extractive industry (OXFAM, 2014). Mining is intensive in the andean region where the dry-land hills prompt significant SY rates even during relatively low rainfall intensities (Michaelides and Martin, 2012).

We argue that the RUSLE-GGS performance for Peru can be improved if engineers/scientists from public agencies use the data they may have access to and set the year 1990 as long-term benchmark to assess ER spatio-temporal gradients. A long-term benchmark would allow for consistent cost-benefit analyses of erosion mitigation strategies (Vanacker et al., 2007). In our opinion, these strategies should include (1) the establishment of a freely available SY database for larger areas in the Peruvian territory, and (2) a consistent program to document sediment fluxes triggered by ENSO events that currently are poorly documented even though they can increase 11 times the fluxes from normal years (Tote et al., 2011). Finally, it is worth to point out that our results suggest that Peru urgently needs regulatory standards to manage its territorial erosion control challenges.

5. Conclusions and implications

The profuse literature review presented in this study indicates that soil erosion in developing countries is a matter of serious concern and that Peru, an upper-middle-income economy, presents erosion features that exemplify such situation. Thus, it is reasonably grounded to state that the quantification of soil erosion rates (ERs) in developing countries needs to be addressed with particular urgency. This is however challenging because they commonly suffer from an inherent paucity of conventional ground-based observations and field relations to obtain ERs.

The Generalized Likelihood Uncertainty Estimation (GLUE) principles have been extensively used to identify behavioral model outputs under conditions where there is an incomplete knowledge of the modeled system and the input data is, at some degree, uncertain. RUSLE-GGS results from the combined application of RUSLE-GIS, GLUE, and sediment delivery ratio (SDR) functions in the following sequence: (1) ER samples are constructed using RUSLE-GIS based on available local/global geoenvironmental observations and field relations, (2) area-specific sediment yield samples are constructed utilizing SDR transfer functions, and (3) the most behavioral samples are assessed by means of bias analysis and cross validation. It is aimed to cope with the technical challenges related to estimating ERs in developing countries at country scale.

RUSLE-GGS is successfully applied to obtain ER and potential erosion maps for Peru at 5-km resolution for the years 1990, 2000 and 2010. For this period, Peru exhibits erosion rates in the order of $24 - 33\ t/h/y$ which are triggered by natural (e.g., ENSO, the Andes) and anthropogenic controls (e.g., changes in land use as its economy relies mainly on extractive industries, expansion of its infrastructure portfolio, urban population growth). Determining which of them is the predominant control certainly deserves further attention. ERs for the year 2000 are possibly underestimated as they include a 1989 strong ENSO event.

Despite its limitations, RUSLE-GGS accounts the model uncertainty. Consequently, we believe that (1) it has the potential to provide the initial standard and systematic frame to quantify erosion rates in developing countries, which can subsequently be used to make institutional decisions to efficiently control soil erosion, and (2) the year 1990 could be set as a benchmark to track the regional evolution of soil erosion in such countries. We also believe that these steps would represent active measures to meet Goal 15 of the UN 2030 agenda.

Supplementary Material

Input data for the creation of ER samples and output of RUSLE-GGS is presented in Rosas and Gutierrez (2017) (`https://doi.pangaea.de/10.1594/PANGAEA.884460`). A file that details the RUSLE-GIS model also accompanies this contribution.

Acknowledgements

This project was funded by CONCYTEC within the framework of the 012-2013-FONDECYT Agreement. The authors started this study under the guidelines of GERDIS-PUCP (Pontificia Universidad Católica del Perú). We would like to thank the Servicio Nacional de Meteorología e Hidrología and the Instituto Geofísico del Perú for providing valuable data for this study. The authors also appreciate the technical discussions with Dr. Waldo Lavado and Dr. Sergio Morera. Dr. Gutierrez thanks to the Universidad del Norte (Barranquilla) for funding the completion of this contribution. Finally, we thank the anonymous reviewers of this manuscript for their valuable comments.

References

Adler, R., Huffman, G., Chang, A., Ferraro, R., Xie, P., Janowiak, J., Rudolf, B., Schneider, U., Curtis, S., Bolvin, D., Gruber, A., Susskind, J., and Arkin, P. (2003). The version 2 global precipitation climatology project (GPCP) monthly precipitation analysis (1979-present). *Journal of Hydrometeorology*, *4*, 1147–1167.

Alatorre, L., Beguería, S., and García-Ruiz, J. M. (2010). Regional scale modeling of hillslope sediment delivery: a case study in the Barasona Reservoir watershed (Spain) using WATEM/SEDEM. *Journal of Hydrology*, *391*, 109–123.

Alcantara-Ayala, I. (2002). Geomorphology, natural hazards, vulnerability and prevention of natural disasters in developing countries. *Geomorphology*, *47*, 107–124.

Alegre, J., and Rao, M. (1996). Soil and water conservation by contour hedging in the humid tropics of Peru. *Agriculture, ecosystems & environment*, *57*, 17–25.

485 Alegre, J. C., and Cassel, D. (1996). Dynamics of soil physical properties under alternative systems
486 to slash-and-burn. *Agriculture, Ecosystems & Environment*, *58*, 39–48.

487 ANA (2010). *Recursos hídricos del Perú en cifras*. Boletín Técnico Autoridad Nacional del Agua.
488 URL: `http://repositorio.ana.gob.pe/handle/ANA/211`.

489 Ananda, J., and Herath, G. (2003). Soil erosion in developing countries: a socio-economic appraisal.
490 *Journal of environmental management*, *68*, 343–353.

491 Aronica, G., Bates, P., and Horritt, M. (2002). Assessing the uncertainty in distributed model
492 predictions using observed binary pattern information within GLUE. *Hydrological Processes*, *16*,
493 2001–2016.

494 Ayele, G. K., Gessess, A. A., Addisie, M. B., Tilahum, S. A., Tebebu, T. Y., Tenessa, D. B.,
495 Langendoen, E. J., Nicholson, C. F., and Steenhuis, T. S. (2015). A biophysical and economics
496 assessment of a community-based rehabilitated gully in the Ethiopian highlands. *Land Degradation*
497 *and Development*, (pp. 270–280).

498 Bellin, N., Vanacker, V., van Wesemael, B., Solé-Benet, A., and Bakker, M. (2011). Natural and
499 anthropogenic controls on soil erosion in the Internal Betic Cordillera (southeast Spain). *Catena*,
500 *87*, 190–200.

501 Betrie, G. D., Mohamed, Y. A., van Griensven, A., and Srinivasan, R. (2011). Sediment management
502 modelling in the Blue Nile Basin using SWAT model. *Hydrology and Earth System Sciences*, *15*,
503 807–818.

504 Beven, K., and Brazier, R. (2011). Dealing with uncertainty in erosion model predictions. In
505 M. R.P.C., and N. M.A. (Eds.), *Handbook of erosion modelling* chapter 4. (pp. 52–79). UK: Wiley
506 Blackwell Publishing. (1st ed.).

507 Beven, K. J., Smith, P. J., and Freer, J. E. (2008). So just why would a modeller choose to be
508 incoherent? *Journal of hydrology*, *354*, 15–32.

509 Bingner, R., Murphree, C., and Mutchler, C. (1989). Comparison of sediment yield models on
510 watersheds in Mississippi. *Transactions of the ASAE*, *32*, 529–0534.

511 Boardman, J. (2006). Soil erosion science: Reflections on the limitations of current approaches.
512 *Catena*, *68*, 73–86.

513 Borrelli, P., Robinson, D. A., Fleischer, L. R., Lugato, E., Ballabio, C., Alewell, C., Meusburger,
514 K., Modugno, S., Schütt, B., Ferro, V. et al. (2017). An assessment of the global impact of 21st
515 century land use change on soil erosion. *Nature communications*, *8*, 2013.

516 Brazier, R. E., Beven, K. J., Anthony, S. G., and Rowan, J. S. (2001). Implications of model
517 uncertainty for the mapping of hillslope-scale soil erosion predictions. *Earth Surface Processes and*
518 *Landforms*, *26*, 1333–1352.

519 Brazier, R. E., Beven, K. J., Freer, J., and Rowan, J. S. (2000). Equifinality and uncertainty in
520 physically based soil erosion models: application of the GLUE methodology to WEPP–the Water
521 Erosion Prediction Project–for sites in the UK and USA. *Earth Surface Processes and Landforms*,
522 *25*, 825–845.

523 Catari, G., Latron, J., and Gallart, F. (2011). Assessing the sources of uncertainty associated with
524 the calculation of rainfall kinetic energy and erosivity-application to the Upper Llobregat Basin,
525 NE Spain. *Hydrology and Earth System Sciences*, *15*, 679.

526 Catari Yujra, G., and Saurí i Pujol, D. (2010). *Assessment of uncertainties of soil erosion and*
527 *sediment yield estimates at two spatial scales in the upper Llobregat basin (SE Pyrenees, Spain)*.
528 Ph.D. thesis Universitat Autònoma de Barcelona,.

529 Cea, L., Legout, C., Grangeon, T., and Nord, G. (2016). Impact of model simplifications on soil
530 erosion predictions: application of the GLUE methodology to a distributed event-based model at
531 the hillslope scale. *Hydrological Processes*, *30*, 1096–1113.

532 Cerdà, A., Brazier, R., Nearing, M., and de Vente, J. (2013). Scales and erosion. *Catena*, *102*, 1–2.
533 Scales in Soil Erosion.

534 Channan, S., Collins, K., and Emanuel, W. R. (2011). *Global mosaics of the standard MODIS land*
535 *cover type data*. College Park, Maryland, USA: University of Maryland and the Pacific Northwest
536 National Laboratory.

Dedkov, A., and Gusarov, A. (2006). Suspended sediment yield from continents into the world ocean: spatial and temporal changeability. In *Sediment Dynamics and the Morphology of Fluvial Systems. IAHS Publication* (pp. 3–11). volume 396.

Doetterl, S., Van Oost, K., and Six, J. (2012). Towards constraining the magnitude of global agricultural sediment and soil organic carbon fluxes. *Earth Surface Processes and Landforms*, *37*, 642–655.

Espinoza, R., Martinez, J.-M., Le Texier, M., Guyot, J.-L., Fraizy, P., Meneses, P. R., and de Oliveira, E. (2012). A study of sediment transport in the Madeira River, Brazil, using MODIS remote-sensing images. *Journal of South American Earth Sciences*, *1*.

Ferro, V., and Porto, P. (2000). Sediment delivery distributed (SEDD) model. *Journal of hydrologic engineering*, *5*, 411–422.

Freer, J., Beven, K., and Ambroise, B. (1996). Bayesian estimation of uncertainty in runoff prediction and the value of data: An application of the GLUE approach. *Water Resources Research*, *32*, 2161–2173.

Ganasri, B., and Ramesh, H. (2016). Assessment of soil erosion by RUSLE model using remote sensing and GIS-A case study of Nethravathi Basin. *Geoscience Frontiers*, *7*, 953–961.

Grauso, S., Pasanisi, F., and Tebano, C. (2018). Assessment of a simplified connectivity index and specific sediment potential in river basins by means of geomorphometric tools. *Geosciences*, *8*, 48.

Hajigholizadeh, M., Melesse, A., and Fuentes, H. (2018). Erosion and sediment transport modelling in shallow waters: A review on approaches, models and applications. *International journal of environmental research and public health*, *15*, 518.

Harden, C. P. (2006). Human impacts on headwater fluvial systems in the northern and central Andes. *Geomorphology*, *79*, 249–263.

Haregeweyn, N., Poesen, J., Verstraeten, G., Govers, G., Vente, J., Nyssen, J., Deckers, J., and Moeyersons, J. (2013). Assessing the performance of a spatially distributed soil erosion and sedi-

ment delivery model (WATEM/SEDEM) in Northern Ethiopia. *Land Degradation & Development*, *24*, 188–204.

Heckmann, T., Cavalli, M., Cerdan, O., Foerster, S., Javaux, M., Lode, E., Smetanová, A., Vericat, D., and Brardinoni, F. (2018). Indices of sediment connectivity: opportunities, challenges and limitations. *Earth-science reviews*, *187*, 77–108.

Houska, T., Multsch, S., Kraft, P., Frede, H.-G., and Breuer, L. (2014). Monte Carlo-based calibration and uncertainty analysis of a coupled plant growth and hydrological model. *Biogeosciences*, *11*, 2069–2082.

Hudson, N. (1993). *Field plots* volume 68. Food & Agriculture Organization.

Huffman, G., Adler, R., Bolvin, D., Gu, G., Nelkin, E., Bowman, K., Hong, Y., Stocker, E., and Wolff, D. (2007). The TRMM multi-satellite precipitation analysis: Quasi-global, multi-year, combined-sensor precipitation estimates at fine scale. *Journal of Hydrometeorology*, *8*, 38–55.

Hui, L., Xiaoling, C., Lim, K. J., Xiaobin, C., and Sagong, M. (2010). Assessment of soil erosion and sediment yield in Liao watershed, Jiangxi province, China, using USLE, GIS, and RS. *Journal of Earth Science*, *21*, 941–953.

Inbar, M., and Llerena, C. A. (2000). Erosion processes in high mountain agricultural terraces in Peru. *Mountain Research and Development*, *20*, 72–79.

INEI (2012). *IV Censo Nacional Agropecuario*. Technical Report Instituto Nacional de Estadística e Informática, Lima, Peru.

INEI (2014). *Perú: Población estimada al 30 de junio y tasa de crecimiento de las ciudades capitales, por departamento, 2014*. Peru: Instituto Nacional de Estadística e Informática.

INEI (2016). *Peru Statistical Summary 2016*. Lima, Peru: Instituto Nacional de Estadística e Informática.

INRENA (1996). *Memoria Descriptiva: Mapa de Erosión de los Suelos del Perú*. Lima, Perú: Ministerio de Agricultura - Instituto Nacional de Recursos Naturales.

587 ISRIC (2013). SoilGrids: an automated system for global soil mapping. Available for download at
588 http://soilgrids1km.isric.org.

589 Ito, A. (2007). Simulated impacts of climate and land-cover change on soil erosion and implication
590 for the carbon cycle, 1901 to 2100. *Geophysical research letters*, *34*.

591 Jetten, V., and Maneta, M. (2011). Calibration of erosion models. In M. R.P.C., and N. M.A. (Eds.),
592 *Handbook of erosion modelling* chapter 3. (pp. 33–51). UK: Wiley Blackwell Publishing. (1st ed.).

593 Kim, M., and Gilley, J. E. (2008). Artificial neural network estimation of soil erosion and nutrient
594 concentrations in runoff from land application areas. *Computers and electronics in agriculture*,
595 *64*, 268–275.

596 Kirkby, M., and Cox, N. (1995). A climatic index for soil erosion potential (CSEP) including seasonal
597 and vegetation factors. *CATENA*, *1-4*, 333–352.

598 Van der Knijff, J., Jones, R., and Montanarella, L. (2000). *Soil erosion risk assessment in Europe*.
599 Technical Report.

600 Labrière, N., Locatelli, B., Laumonier, Y., Freycon, V., and Bernoux, M. (2015). Soil erosion in the
601 humid tropics: A systematic quantitative review. *Agriculture, Ecosystems & Environment*, *203*,
602 127–139.

603 Lal, R., Delgado, J., Groffman, P., Millar, N., Dell, C., and Rotz, A. (2011). Management to mitigate
604 and adapt to climate change. *Journal of Soil and Water Conservation*, *66*, 276–285.

605 Laraque, A., Bernal, C., Bourrel, L., Darrozes, J., Christophoul, F., Armijos, E., Fraizy, P., Pombosa,
606 R., and Guyot, J.-L. (2009). Sediment budget of the Napo river, Amazon basin, Ecuador and Peru.
607 *Hydrological Processes*, *23*, 3509–3524.

608 Latham, J., Cumani, R., Rosati, I., and Bloise, M. (2014). *Global Land Cover SHARE database Beta-*
609 *Release Version 1.0*. Rome, Italy: Food and Agriculture Organization of the United Nations,FAO.

610 Latrubesse, E. M., and Restrepo, J. D. (2014). Sediment yield along the Andes: continental budget,

regional variations, an comparisons with other basins from orogenic mountain belts. *Geomorphology*, *216*, 225–233.

Lee, M., Yu, I., Necesito, I. V., Kim, H., and Jeong, S. (2014). Estimation of sediment yield using total sediment yield formulas and RUSLE. *Journal of the Korean Society of Hazard Mitigation*, *14*, 279–288.

Loveland, T., Reed, B., Brown, J., Ohlen, D., Zhu, J., Yang, L., and Merchant, J. (2000). Development of a Global Land Cover Characteristics Database and IGBP DISCover from 1-km AVHRR Data. *International Journal of Remote Sensing*, *21*, 303–330.

Lu, Y., Nakicenovic, N., Visbeck, M., and Stevance, A.-S. (2015). Five priorities for the UN Sustainable Development Goals. *Nature*, *520*, 432–433.

Martin-Fernandez, L., and Martinez-Nuñez, M. (2011). A empirical approach to estimate soil erosion risk in Spain. *Sciences of the Total Environment*, *409*, 3114–3123.

Matos, J. (2012). *Estado desbordado y sociedad nacional emergente*. Lima: Centro de Investigación de la Universidad Ricardo Palma.

McCool, D. K., and Busacca, A. J. (1998). Measuring and modeling soil erosion and erosion damages. In *Conservation farming in the United States: The methods and accomplishments of the STEEP program. CRC Press, Boca Raton, FL. Measuring and modeling soil erosion and erosion damages* (pp. 23–56). CRC.

Merritt, W., Letcher, R., and Jakeman, A. (2003). A review of erosion and sediment transport models. *Environmental Modelling and Software*, *18*, 761–799.

METI and NASA (2011). ASTER Global Digital Elevation Model (ASTER GDEM). Available for download at http://gdem.ersdac.jspacesystems.or.jp/.

Michaelides, K., and Martin, G. J. (2012). Sediment transport by runoff on debris-mantled dryland hillslopes. *Journal of Geophysical Research: Earth Surface*, *117*.

635 Millward, A. A., and Mersey, J. E. (1999). Adapting the RUSLE to model soil erosion potential in
636 a mountainous tropical watershed. *Catena*, *38*, 109–129.

637 MINAR (2015). *Informe de Seguimiento Agroeconómico I Trimestre 2015*. Lima, Peru: Ministerio
638 de Agricultura y Riego - Dirección general de seguimiento y evaluación de políticas.

639 Molina, A., Govers, G., Poesen, J., Van Hemelryck, H., De Bièvre, B., and Vanacker, V. (2008).
640 Environmental factors controlling spatial variation in sediment yield in a central Andean mountain
641 area. *Geomorphology*, *98*, 176–186.

642 Mondal, A., Khare, D., Kundu, S., Mukherjee, S., Mukhopadhyay, A., and Mondal, S. (2017).
643 Uncertainty of soil erosion modelling using open source high resolution and aggregated DEMs.
644 *Geoscience Frontiers*, *8*, 425–436.

645 Montgomery, D. R. (2007). Soil erosion and agricultural sustainability. *Proceedings of the National*
646 *Academy of Sciences*, *104*, 13268–13272.

647 Morera, S. B., Condom, T., Vauchel, P., Guyot, J.-L., Galvez, C., , and Crave, A. (2013). Pertinent
648 spatio-temporal scale of observation to understand suspended sediment yield control factors in the
649 Andean region: the case of the Santa River (Peru). *Hydrology and Earth System Sciences*, *17*,
650 4641–4657.

651 Morgan, R., and Nearing, M. (2011). *Handbook of Erosion Modelling*. UK: Wiley-Blackwell.

652 Naipal, V., Reick, C., Pongratz, J., and Van Oost, K. (2015). Improving the global applicability of
653 the RUSLE model adjustment of the topographical and rainfall erosivity factors. *Geoscientific*
654 *Model Development*, *8*, 2893–2913.

655 Nearing, M. (2004). Capabilities and limitations of erosion models and data. In *Proceedings of the*
656 *13th International Soil Conservation Organization Conference, Brisbane, Australia* (pp. 4–8).

657 Nearing, M., Pruski, F., and O'neal, M. (2004). Expected climate change impacts on soil erosion
658 rates: A review. *Journal of soil and water conservation*, *59*, 43–50.

659 Olson, D. M., Dinerstein, E., Wikramanayake, E. D., Burgess, N. D., Powell, G. V., Underwood,
660 E. C., D'amico, J. A., Itoua, I., Strand, H. E., Morrison, J. C. et al. (2001). Terrestrial ecoregions
661 of the World: A new map of life on Earth: A new global map of terrestrial ecoregions provides an
662 innovative tool for conserving biodiversity. *BioScience*, *51*, 933–938.

663 Onyando, J., Kisoyan, P., and Chemelil, M. (2005). Estimation of potential soil erosion for River
664 Perkerra catchment in Kenya. *Water Resources Management*, *19*, 133–143.

665 ORNL-DAAC (2011). 8 km Global Land Cover Data Set Derived from AVHRR. Available for
666 download at http://webmap.ornl.gov/wcsdown/index.jsp.

667 OXFAM (2014). *Geographies of conflict: Mapping overlaps between extractive industries and agri-*
668 *cultural land uses in Ghana and Peru*. Technical Report OXFAM America USA.

669 Panagos, P., Borrelli, P., Poesen, J., Ballabio, C., Lugato, E., Meusburger, K., Montanarella, L., and
670 Alewell, C. (2015). The new assessment of soil loss by water erosion in Europe. *Environmental*
671 *Science & Policy*, *54*, 438–447.

672 Paulet, M., and Amat, C. (1999). *La conservación de suelos en la sierra de Perú. Sistematización de*
673 *la experiencia de Pronamachs en la lucha contra la desertificación*. Lima, Peru: IIICA Consorcio
674 técnico.

675 Peel, M. C., Finlayson, B. L., and McMahon, T. A. (2007). Updated world map of the Köppen-Geiger
676 climate classification. *Hydrology and earth system sciences discussions*, *4*, 439–473.

677 Pepin, E., Guyot, J.-L., Armijos, E., Bazan, H., Fraizy, P., Moquet, J., Noriega, L., Lavado, W.,
678 Pombosa, R., and Vauchel, P. (2013). Climatic control on eastern Andean denudation rates
679 (Central Cordillera from Ecuador to Bolivia). *Journal of South American Earth Sciences*, *44*,
680 85–93.

681 Peucker-Ehrenbrink, B. (2009). Land2sea database of river drainage basin sizes, annual water dis-
682 charges, and suspended sediment fluxes. *Geochemistry, Geophysics, Geosystems*, *10*.

683 Pham, T. N., Yang, D., Kanae, S., Oki, T., and Musiake, K. (2001). Application of RUSLE model
684 on global soil erosion estimate. *Annual Journal of Hydraulic Engineering*, *45*, 811–816.

Pimentel, D., Harvey, C., Resosudarmo, P., Sinclair, K., Kurz, D., McNair, M., Crist, S., Shpritz, L., Fitton, L., Saffouri, R. et al. (1995). Environmental and economic costs of soil erosion and conservation benefits. *Science*, *267*, 1117–1122.

Quinn, W. H., Neal, V. T., and Antunez De Mayolo, S. E. (1987). El Niño occurrences over the past four and a half centuries. *Journal of Geophysical Research*, *92*, 14449–14461.

Quinton, J., Krueger, T., Freer, J., Bilotta, G., and Brazier, R. (2011). A case study of uncertainty: applying GLUE to EUROSEM. In M. R.P.C., and N. M.A. (Eds.), *Handbook of erosion modelling* chapter 5. (pp. 80–97). UK: Wiley Blackwell Publishing. (1st ed.).

Ramankutty, N., Evan, A., Monfreda, C., and Foley, J. (2008). Farming the planet: 1. Geographic distribution of global agricultural lands in the year 2000. *Global Biogeochemical Cycles*, *22*, 1–19.

Ranzi, R., Le, T. H., and Rulli, M. C. (2012). A RUSLE approach to model suspended sediment load in the Lo river (Vietnam): Effects of reservoirs and land use changes. *Journal of Hydrology*, *422*, 17–29.

Renard, K. G., and Freimund, J. R. (1994). Using monthly precipitation data to estimate the R-factor in the revised USLE. *Journal of Hydrology*, *157*, 287–306.

Renfro, G. W. (1975). Use of erosion equations and sediment-delivery ratios for predicting sediment yield. In *Present and prospective technology for predicting sediment yields and sources* (pp. 33–45). USDA-Agricultural Research Washington.

Ribaudo, M. O. (2009). Non-point pollution regulation approaches in the US. In J. Albiac, and A. Dinar (Eds.), *The Management of Water Quality and Irrigation Technologies* chapter 5. (pp. 83–102). London, UK: Earthscan. (1st ed.).

Romero, C. C., Stroosnijder, L., and Baigorria, G. A. (2007). Interrill and rill erodibility in the northern Andean Highlands. *Catena*, *70*, 105–113.

Rosas, M., and Gutierrez, R. R. (2017). Soil erosion rate maps for Peru. URL: https://doi.org/10.1594/PANGAEA.884460. doi:10.1594/PANGAEA.884460.

Sachs, J. D. (2001). *Tropical underdevelopment*. Working Paper 8119 National Bureau of Economic Research. doi:10.3386/w8119.

Salinas, J. L., Kiss, A., Viglione, A., Viertl, R., and Blöschl, G. (2016). A fuzzy bayesian approach to flood frequency estimation with imprecise historical information. *Water Resources Research*, .

Scheidegger, A. (1992). Limitations of the system approach in geomorphology. *Geomorphology*, *5*, 213–217.

Scheidegger, A., and Ai, N. (1986). Tectonic process and geomorphological design. *Tectonophysics*, *126*, 285–300.

Shamshad, A., Leow, C., Ramlah, A., Wan Hussin, W., and Mohd. Sanusi, S. (2008). Applications of AnnAGNPS model for soil loss estimation and nutrient loading for Malaysian conditions. *International Journal of Applied Earth Observation and Geoinformation*, *10*, 239–252.

Sharda, V. N., and Ojasvi, P. R. (2016). A revised soil erosion budget for India: role of reservoir sedimentation and land-use protection measures. *Earth Surface Processes and Landforms*, *41*, 2007–2023.

Showstack, R. (2015). Group pushes for using earth observations in decision making. *EOS*, *96*.

Singh, G., and Panda, R. K. (2017). Grid-cell based assessment of soil erosion potential for identification of critical erosion prone areas using USLE, GIS and remote sensing: A case study in the Kapgari watershed, India. *International Soil and Water Conservation Research*, *5*, 202–211.

Skeldon, R. (1977). The evolution of migration patterns during urbanization in Peru. *Geographical review*, (pp. 394–411).

Šúri, M., Cebecauer, T., Hofierka, J., and Fulajtár, E. (2002). Erosion assessment of Slovakia at regional scale using gis. *Ecology*, *21*, 404–422.

Swarnkar, S., Malini, A., Tripathi, S., and Sinha, R. (2017). Assessment of uncertainties in soil erosion and sediment yield estimates at ungauged basins: An application to the Garra River basin, India. *Hydrology and Earth System Sciences Discussions*, *2017*, 1–31.

735 Syvitski, J. P., and Milliman, J. D. (2007). Geology, Geography, and humans battle for dominance
736 over the delivery of fluvial sediment to the coastal ocean. *The Journal of Geology*, *115*, 1–19.

737 Takahashi, K., Montecinos, A., Goubanova, K., and Dewitte, B. (2011). ENSO regimes: Reinter-
738 preting the Canonical and Modoki El Niño. *Geophysical Research Letters*, *38*. L10704.

739 Terranova, O., Antronico, L., Coscarelli, R., and Iaquinta, P. (2009). Soil erosion risk scenarios in the
740 Mediterranean environment using RUSLE and GIS: an application model for Calabria (southern
741 Italy). *Geomorphology*, *112*, 228–245.

742 Tote, C., Govers, G., Van Kerckhoven, S., Filiberto, I., Verstraeten, G., and Eerens, H. (2011). Effect
743 of ENSO events on sediment production in a large coastal basin in northern Peru. *Earth Surface*
744 *Processes and Landforms*, *36*, 1776–1788.

745 United Nations (2015). *Resolution adopted by the General Assembly on 25 September 2015. Trans-*
746 *forming our world: the 2030 Agenda for Sustainable Development*. Technical Report United Na-
747 tions - General Assembly USA.

748 USDA-NRCS (1979). Sediment sources, yields, and delivery ratios. In *National Engineering Hand-*
749 *book, Section 3, Sedimentation* (p. 120).

750 Van Oost, K., Quine, T., Govers, G., De Gryze, S., Six, J., Harden, J., Ritchie, J., McCarty, G.,
751 Heckrath, G., Kosmas, C. et al. (2007). The impact of agricultural soil erosion on the global carbon
752 cycle. *Science*, *318*, 626–629.

753 Vanacker, V., von Blanckenburg, F., Govers, G., Molina, A., Poesen, J., Deckers, J., and Kubik, P.
754 (2007a). Restoring dense vegetation can slow mountain erosion to near natural benchmark levels.
755 *Geology*, *35*, 303–306.

756 Vanacker, V., Molina, A., Govers, G., Poesen, J., and Deckers, J. (2007b). Spatial variation of
757 suspended sediment concentrations in a tropical Andean river system: The Paute River, southern
758 Ecuador. *Geomorphology*, *87*, 53–67.

759 Vanoni, V. A. (1975). *Sedimentation engineering, ASCE Manuals and Reports on Engineering Prac-*
760 *tice No. 54*. Technical Report.

761 de Vente, J., Poesen, J., and Verstraeten, G. (2005). The application of semi-quantitative methods
762 and reservoir sedimentation rates for the prediction of basin sediment yield in Spain. *Journal of*
763 *Hydrology*, *305*, 63–86.

764 de Vente, J., Poesen, J., Verstraeten, G., Govers, G., Vanmaercke, M., Van Rompaey, A., Arabkhedri,
765 M., and Boix-Fayos, C. (2013). Predicting soil erosion and sediment yield at regional scales: Where
766 do we stand? *Earth-Science Reviews*, (pp. 16 – 29).

767 de Vente, J., Poesen, J., Verstraeten, G., Van Rompaey, A., and Govers, G. (2008). Spatially
768 distributed modelling of soil erosion and sediment yield at regional scales in Spain. *Global and*
769 *Planetary Change*, *60*, 393–415.

770 Vigiak, O., Borselli, L., Newham, L., McInnes, J., and Roberts, A. (2012). Comparison of conceptual
771 landscape metrics to define hillslope-scale sediment delivery ratio. *Geomorphology*, *138*, 74–88.

772 Vuille, M., Francou, B., Wagnon, P., Juen, I., Kaser, G., Mark, B. G., and Bradley, R. S. (2008).
773 Climate change and tropical Andean glaciers: Past, present and future. *Earth-Science Reviews*,
774 *89*, 70–96.

775 Vuohelainen, A. J., Coad, L., Marthews, T. R., Malhi, Y., and Killeen, T. J. (2012). The effectiveness
776 of contrasting protected areas in preventing deforestation in Madre de Dios, Peru. *Environmental*
777 *Management*, *50*, 645–663. doi:10.1007/s00267-012-9901-y.

778 Wei, H., Nearing, M. A., Stone, J. J., and Breshears, D. D. (2008). A dual Monte Carlo approach
779 to estimate model uncertainty and its application to the rangeland hydrology and erosion model.
780 *Transactions of the ASABE*, *51*, 515–520.

781 Williams, J. R. (1977). Sediment-yield prediction with universal equation using runoff energy factor.
782 In USDA-ARS (Ed.), *Present and Prospective Technology for Predicting Sediment Yields and*
783 *Sources: Proceedings of the Sediment-Yield Workshop* (pp. 244–252). USDA-ARS.

784 Williams, J. R., and Berndt, H. D. (1972). Sediment yield computed with universal equation. *Journal*
785 *of the Hydraulics Division*, *98*, 2087–2098.

World Bank (2009). *Peru - Country note on climate change aspects in agriculture*. Climate change aspects in agriculture country note brief World Bank Washington, DC. URL: http://documents.worldbank.org/curated/en/614951468299112368/Peru-Country-note-on-clima

World Bank (2015). *World Development Indicators: Agricultural inputs*. Technical Report The World Bank Group USA.

Yang, D., Kanae, S., Oki, T., Koike, T., and Musiake, K. (2003). Global potential soil erosion with reference to land use and climate changes. *Hydrological processes*, *17*, 2913–2928.

Figure 1

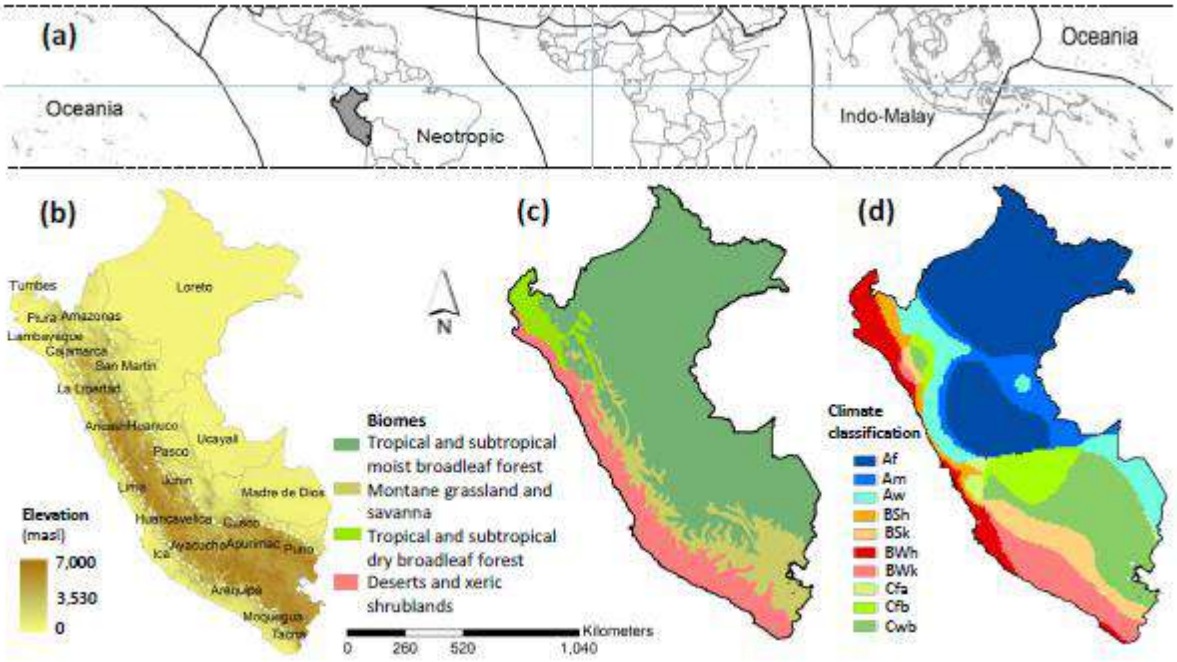
(a)
Oceania
Neotropic
Indo-Malay
Oceania
(b)
Tumbes
Loreto
Piura
Amazonas
Lambayeque
Cajamarca
San Martin
La Libertad
Ancash
Huanuco
Ucayali
Pasco
Junin
Lima
Madre de Dios
Huancavelica
Cusco
Ayacucho
Apurimac
Puno
Ica
Arequipa
Moquegua
Tacna
Elevation
(masl)
7,000
3,530
0
N
(c)
Biomes
Tropical and subtropical moist broadleaf forest
Montane grassland and savanna
Tropical and subtropical dry broadleaf forest
Deserts and xeric shrublands
0
260
520
1,040
Kilometers
(d)
Climate classification
Af
Am
Aw
BSh
BSk
BWh
BWk
Cfa
Cfb
Cwb

Figure 2

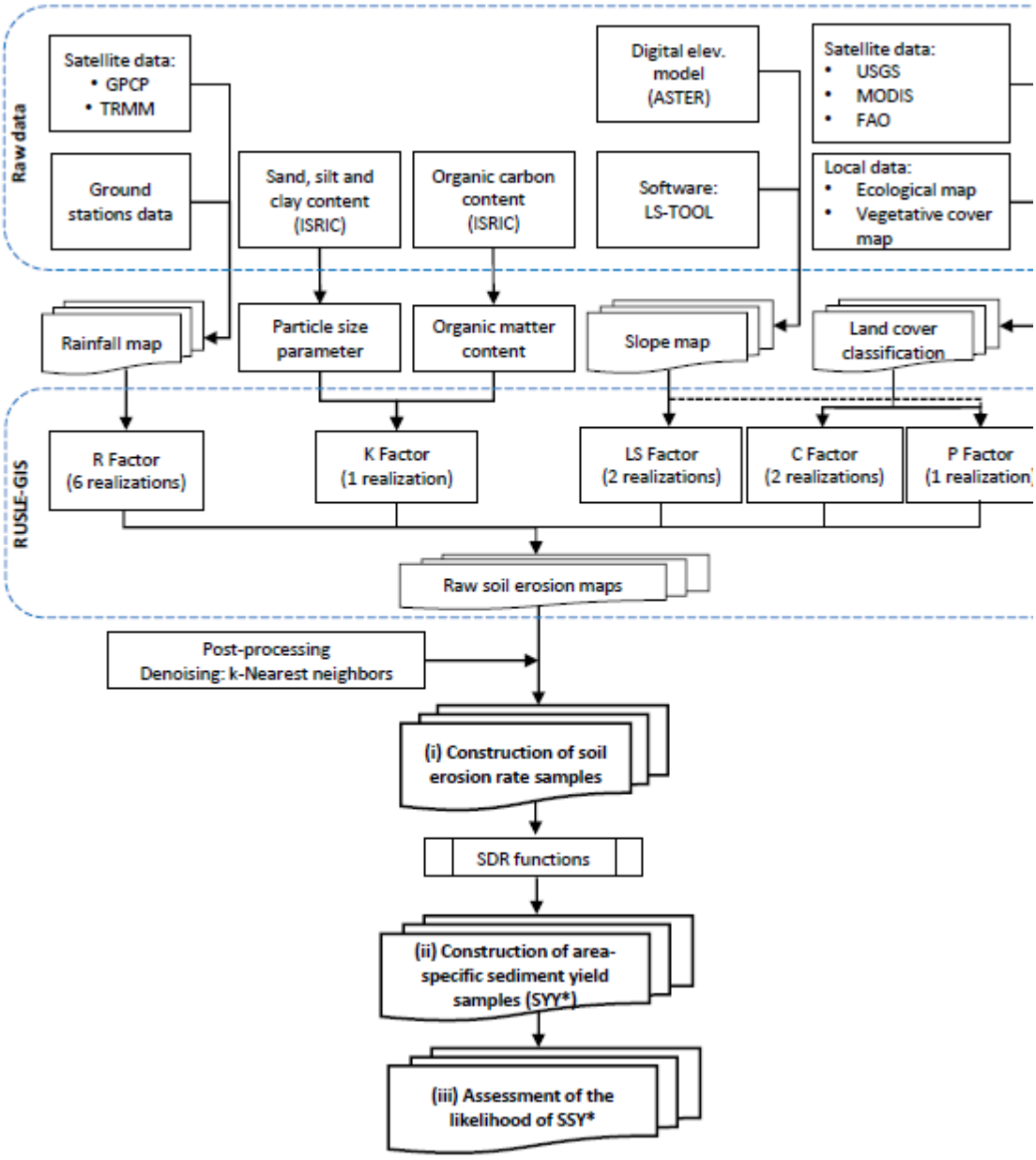
Raw data
Satellite data:
• GPCP
• TRMM
Ground stations data
Sand, silt and clay content (ISRIC)
Organic carbon content (ISRIC)
Digital elev. model (ASTER)
Software: LS-TOOL
Satellite data:
• USGS
• MODIS
• FAO
Local data:
• Ecological map
• Vegetative cover map
Rainfall map
Particle size parameter
Organic matter content
Slope map
Land cover classification
RUSLE-GIS
R Factor (6 realizations)
K Factor (1 realization)
LS Factor (2 realizations)
C Factor (2 realizations)
P Factor (1 realization)
Raw soil erosion maps
Post-processing
Denoising: k-Nearest neighbors
(i) Construction of soil erosion rate samples
SDR functions
(ii) Construction of area-specific sediment yield samples (SYY*)
(iii) Assessment of the likelihood of SSY*

Figure 3

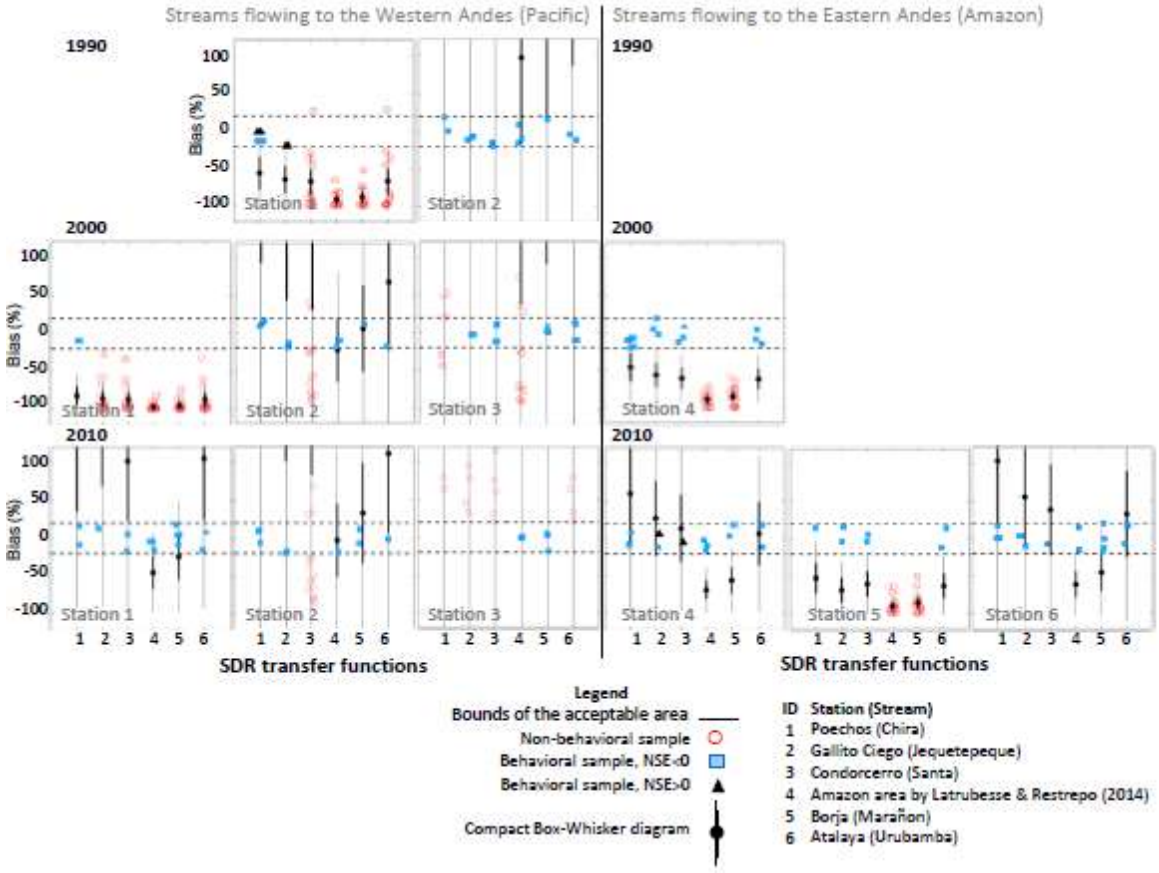
Streams flowing to the Western Andes (Pacific)
Streams flowing to the Eastern Andes (Amazon)
1990
2000
2010
Bias (%)
Station 1
Station 2
Station 3
Station 4
Station 5
Station 6
SDR transfer functions
Legend
Bounds of the acceptable area
Non-behavioral sample
Behavioral sample, NSE<0
Behavioral sample, NSE>0
Compact Box-Whisker diagram
ID Station (Stream)
1 Poechos (Chira)
2 Gallito Ciego (Jequetepeque)
3 Condorcerro (Santa)
4 Amazon area by Latrubesse & Restrepo (2014)
5 Borja (Marañon)
6 Atalaya (Urubamba)

Figure 4

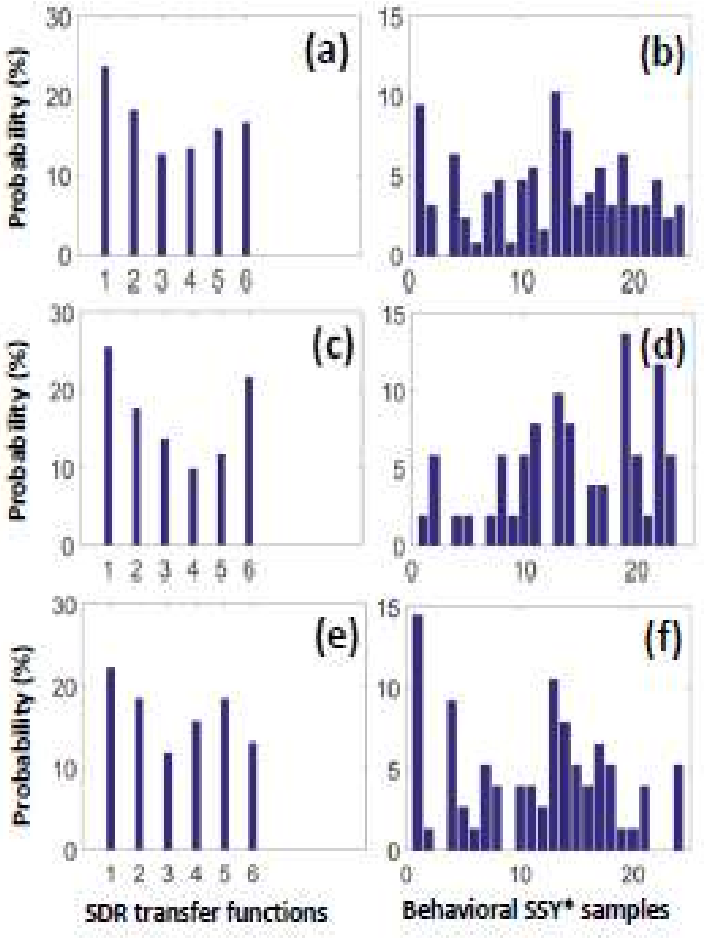
(a)
(b)
(c)
(d)
(e)
(f)
Probability (%)
SDR transfer functions
Behavioral SSY* samples

Figure 5

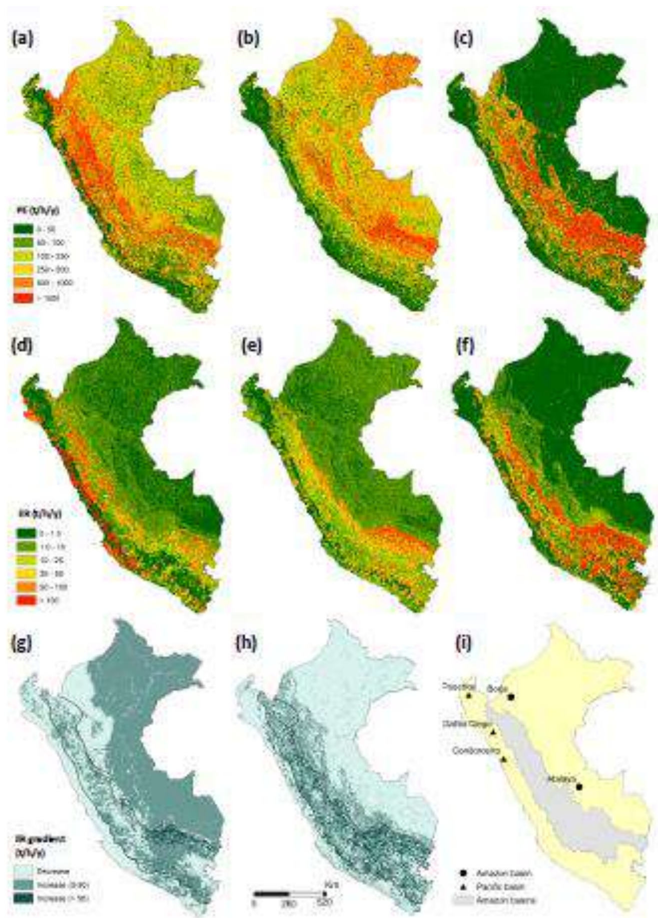

Figure 6

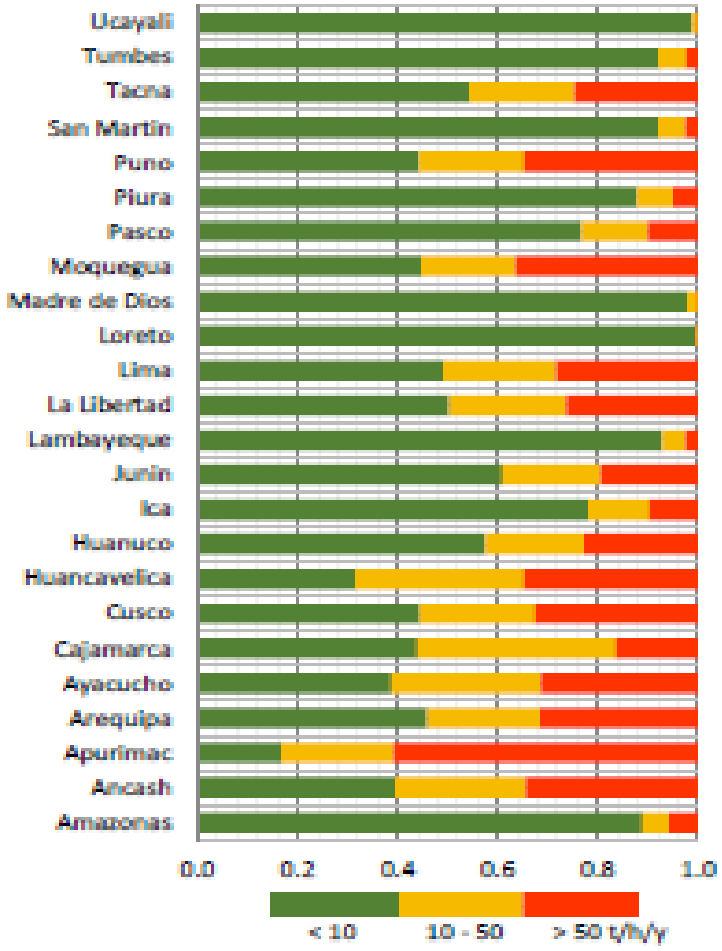
Ucayali
Tumbes
Tacna
San Martin
Puno
Piura
Pasco
Moquegua
Madre de Dios
Loreto
Lima
La Libertad
Lambayeque
Junin
Ica
Huanuco
Huancavelica
Cusco
Cajamarca
Ayacucho
Arequipa
Apurimac
Ancash
Amazonas
0.0
0.2
0.4
0.6
0.8
1.0
< 10
10 - 50
> 50 t/h/y

GRAPHICAL ABSTRACT

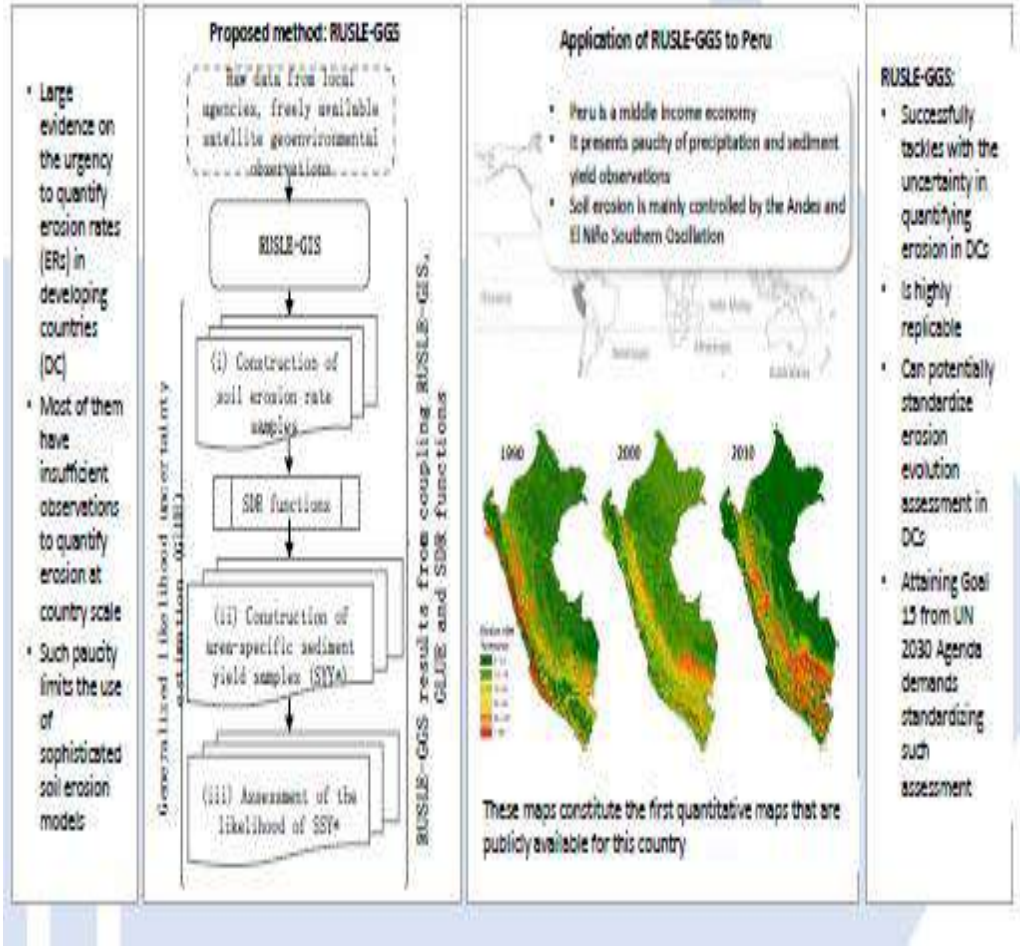

HIGHLIGHTS

- Large evidence on the urgency to asses soil erosion in developing countries (DC)
- Most DC have insufficient observations to quantify erosion at country scale
- RUSLE-GGS successfully tackles with the uncertainty in quantifying erosion in DC
- RUSLE-GGS can potentially standardize erosion evolution assessment in DC
- Attaining Goal 15 from UN 2030 Agenda demands standardizing such assessment

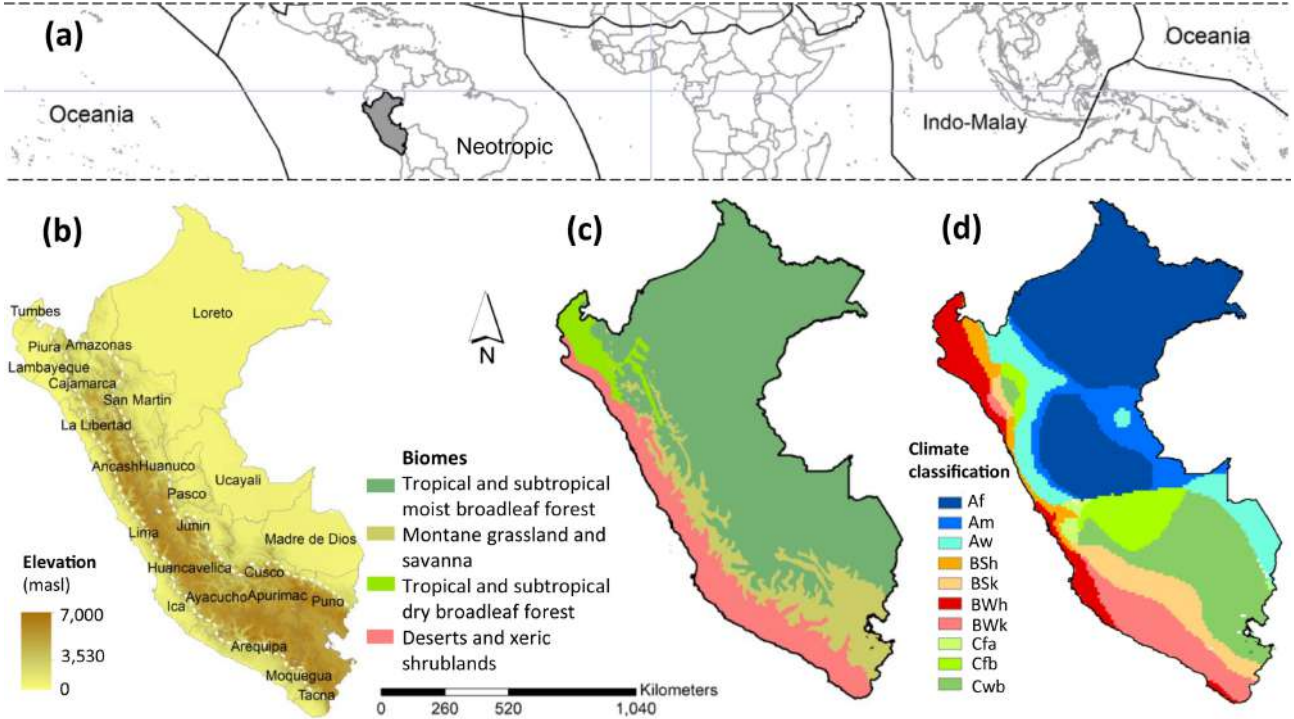
(a)
Oceania
Neotropic
Indo-Malay
Oceania
(b)
Tumbes
Loreto
Piura
Amazonas
Lambayeque
Cajamarca
San Martin
La Libertad
AncashHuanuco
Ucayali
Pasco
Junin
Lima
Madre de Dios
Huancavelica
Cusco
Ayacucho
Apurimac
Puno
Ica
Arequipa
Moquegua
Tacna
Elevation
(masl)
7,000
3,530
0
N
(c)
Biomes
Tropical and subtropical moist broadleaf forest
Montane grassland and savanna
Tropical and subtropical dry broadleaf forest
Deserts and xeric shrublands
0
260
520
1,040
Kilometers
(d)
Climate classification
Af
Am
Aw
BSh
BSk
BWh
BWk
Cfa
Cfb
Cwb

Figure 1

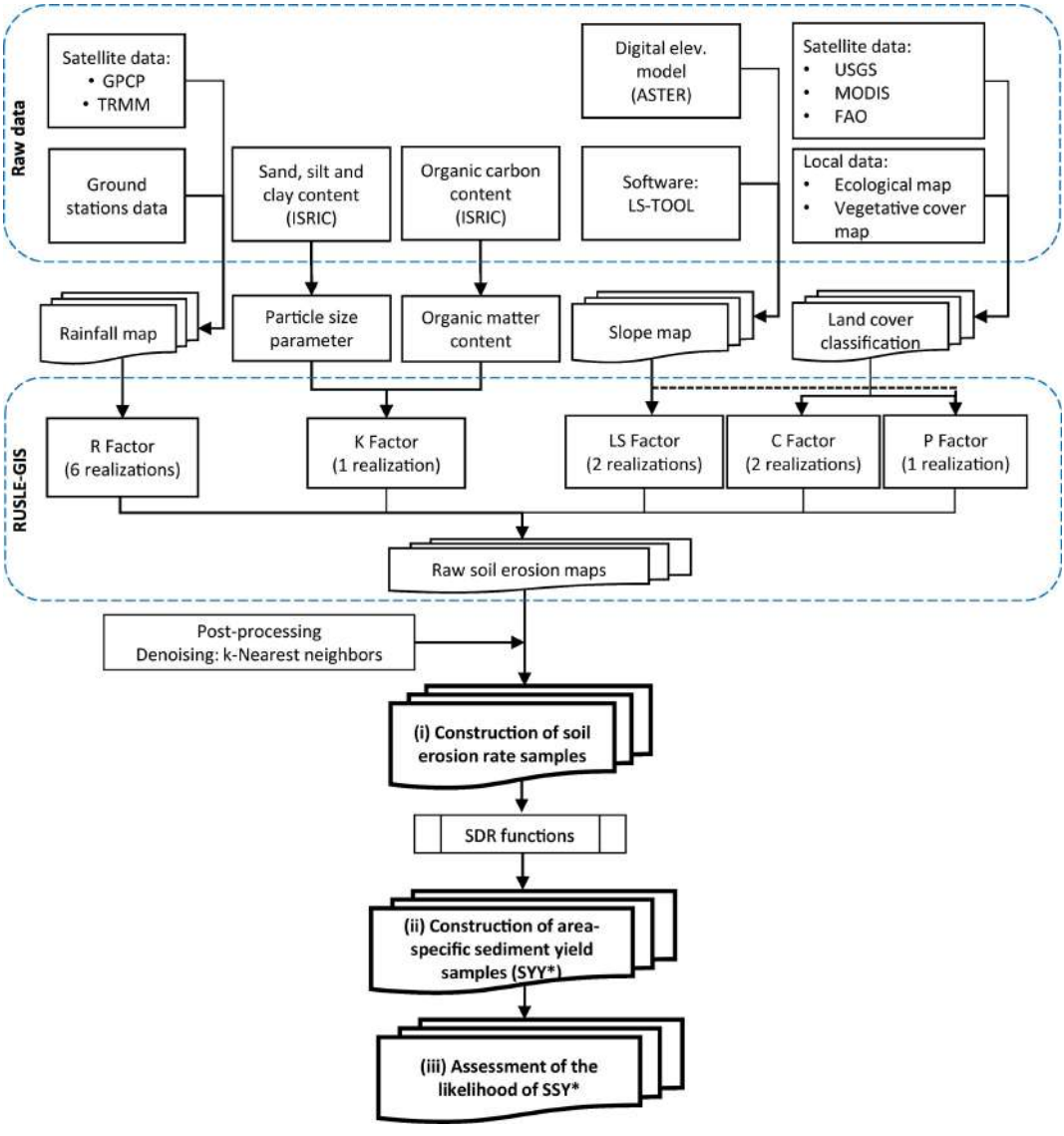
Raw data
Satellite data:
• GPCP
• TRMM
Digital elev. model (ASTER)
Satellite data:
• USGS
• MODIS
• FAO
Ground stations data
Sand, silt and clay content (ISRIC)
Organic carbon content (ISRIC)
Software: LS-TOOL
Local data:
• Ecological map
• Vegetative cover map
Rainfall map
Particle size parameter
Organic matter content
Slope map
Land cover classification
RUSLE-GIS
R Factor (6 realizations)
K Factor (1 realization)
LS Factor (2 realizations)
C Factor (2 realizations)
P Factor (1 realization)
Raw soil erosion maps
Post-processing
Denoising: k-Nearest neighbors
(i) Construction of soil erosion rate samples
SDR functions
(ii) Construction of area-specific sediment yield samples (SYY*)
(iii) Assessment of the likelihood of SSY*

Figure 2

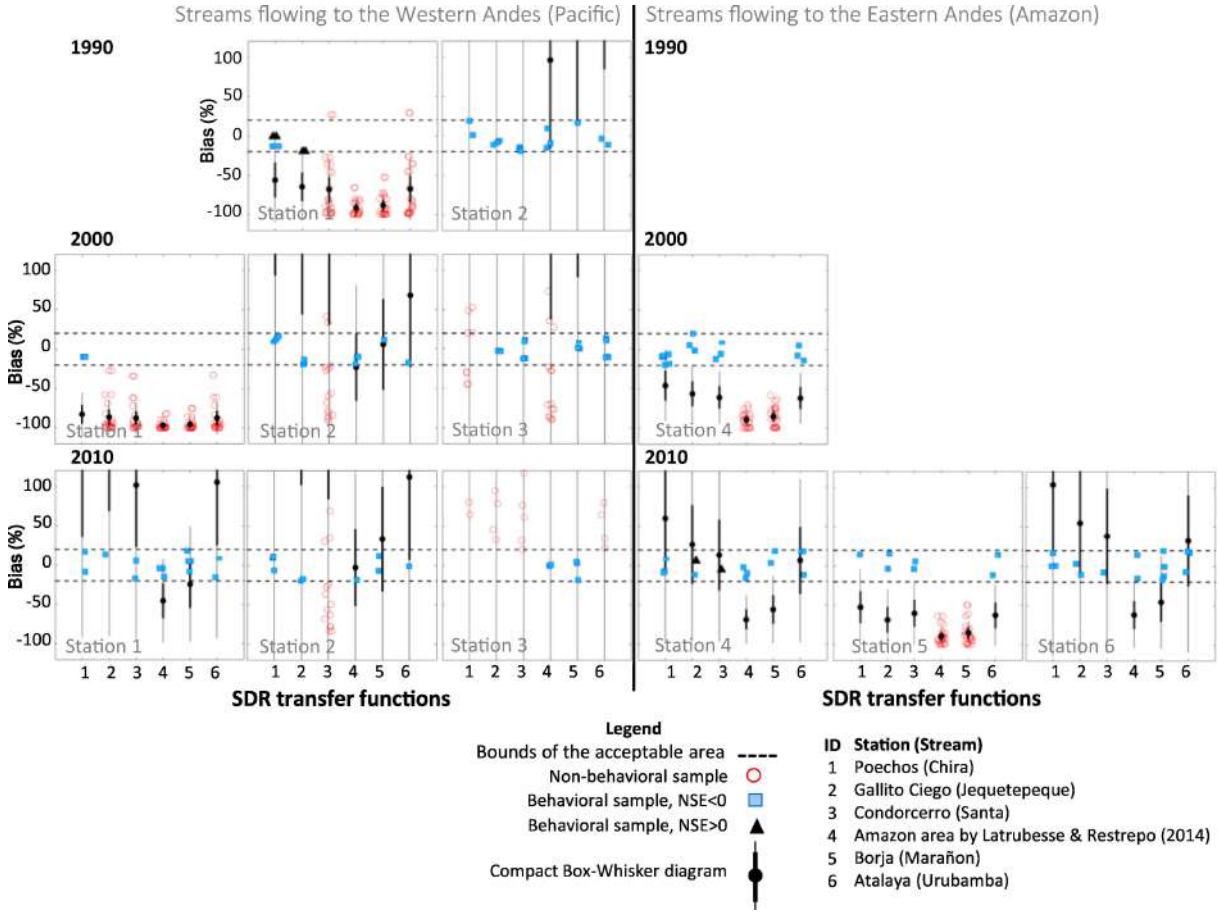
Streams flowing to the Western Andes (Pacific)
Streams flowing to the Eastern Andes (Amazon)
1990
2000
2010
Bias (%)
100
50
0
-50
-100
Station 1
Station 2
Station 3
Station 4
Station 5
Station 6
1 2 3 4 5 6
SDR transfer functions
Legend
Bounds of the acceptable area
Non-behavioral sample
Behavioral sample, NSE<0
Behavioral sample, NSE>0
Compact Box-Whisker diagram
ID Station (Stream)
1 Poechos (Chira)
2 Gallito Ciego (Jequetepeque)
3 Condorcerro (Santa)
4 Amazon area by Latrubesse & Restrepo (2014)
5 Borja (Marañon)
6 Atalaya (Urubamba)

Figure 3

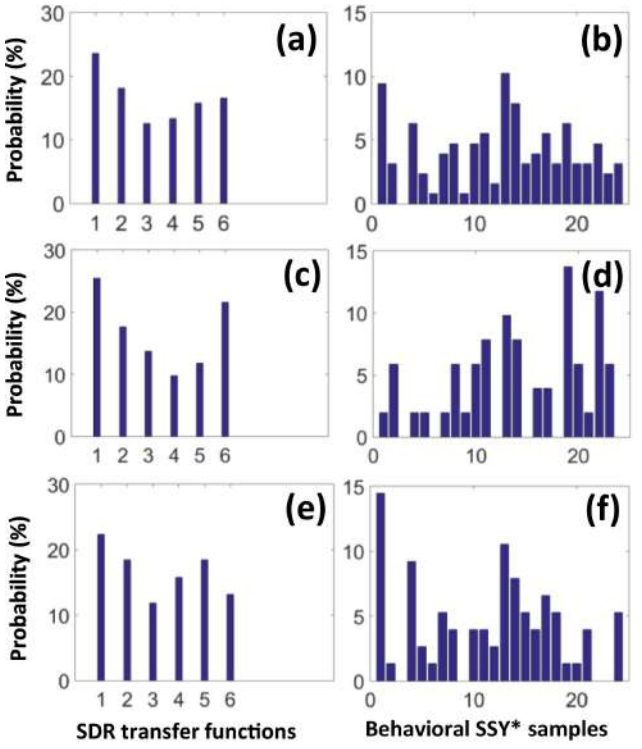
(a)
(b)
(c)
(d)
(e)
(f)
Probability (%)
Probability (%)
Probability (%)
SDR transfer functions
Behavioral SSY* samples

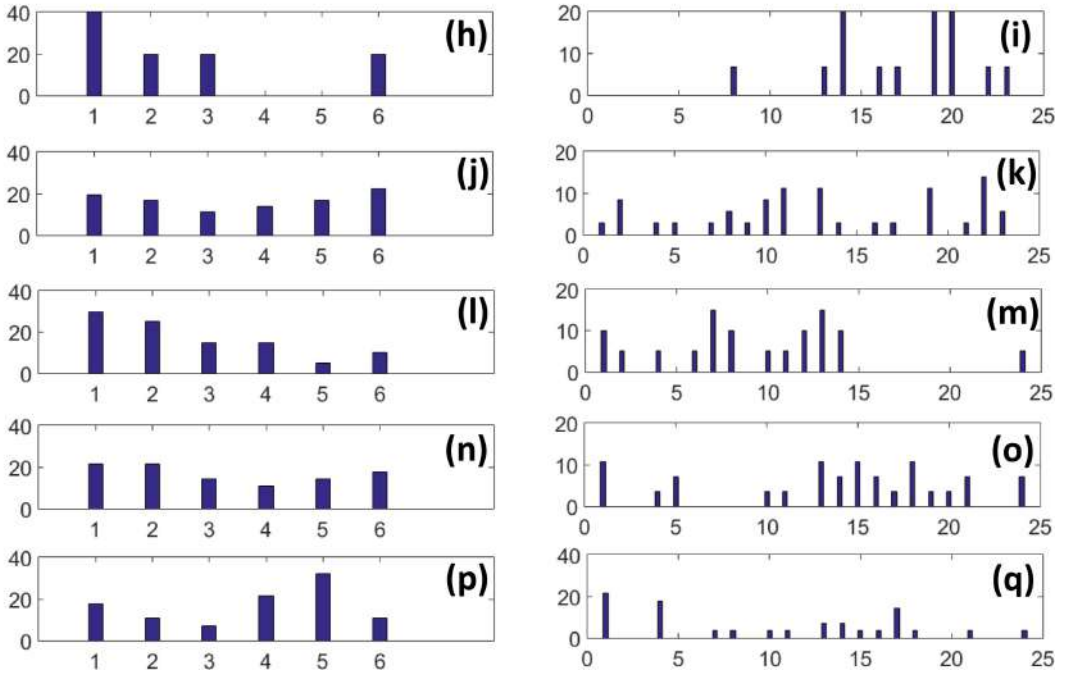
(h)
(i)
(j)
(k)
(l)
(m)
(n)
(o)
(p)
(q)

Figure 4

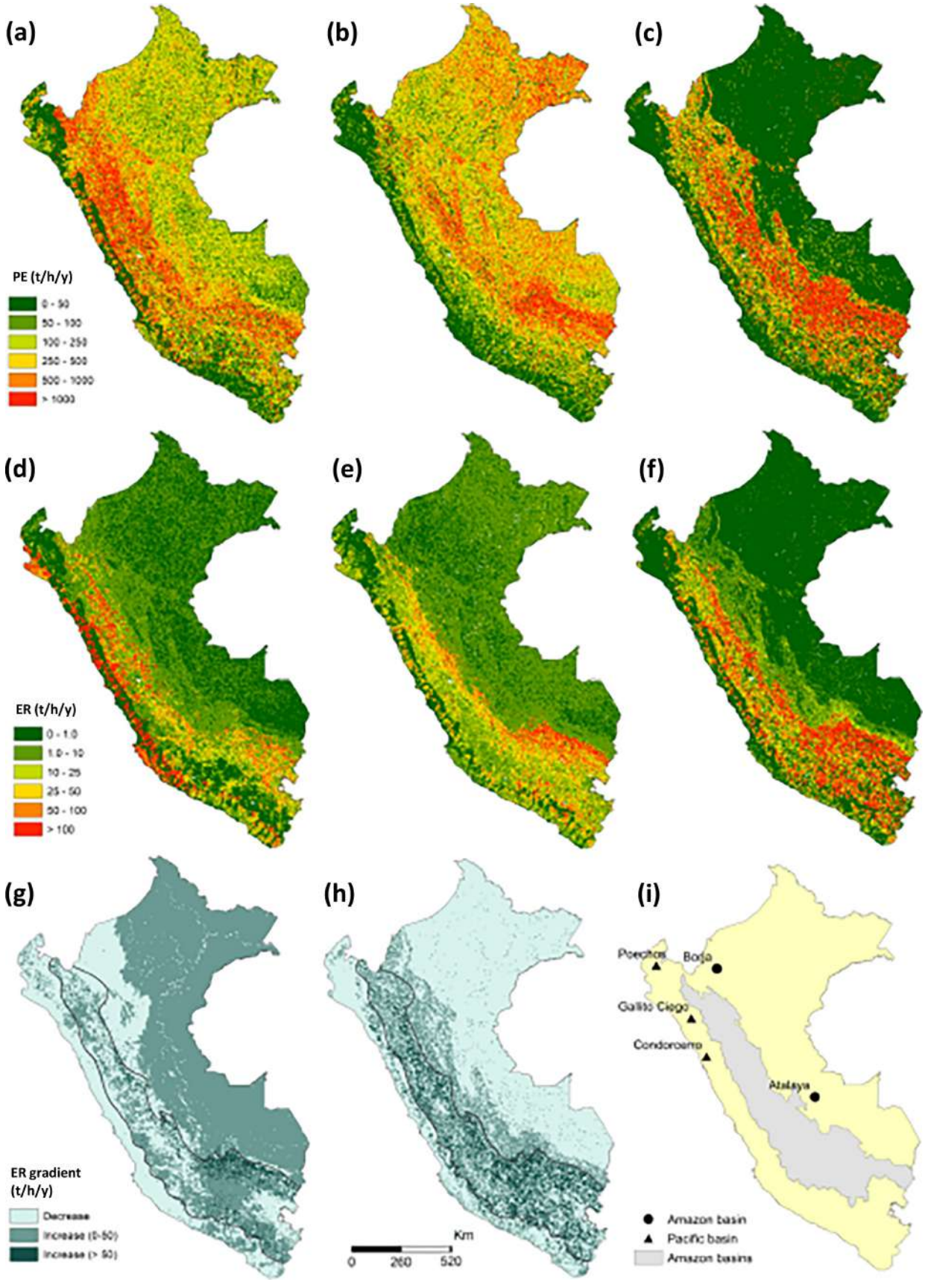
(a)
(b)
(c)
PE (t/h/y)
0 - 50
50 - 100
100 - 250
250 - 500
500 - 1000
> 1000
(d)
(e)
(f)
ER (t/h/y)
0 - 1.0
1.0 - 10
10 - 25
25 - 50
50 - 100
> 100
(g)
(h)
(i)
ER gradient (t/h/y)
Decrease
Increase (0-50)
Increase (> 50)
Km
0
260
520
Porcheos
Borja
Gallito Ciego
Condorcanqui
Atalaya
Amazon basin
Pacific basin
Amazon basins

Figure 5

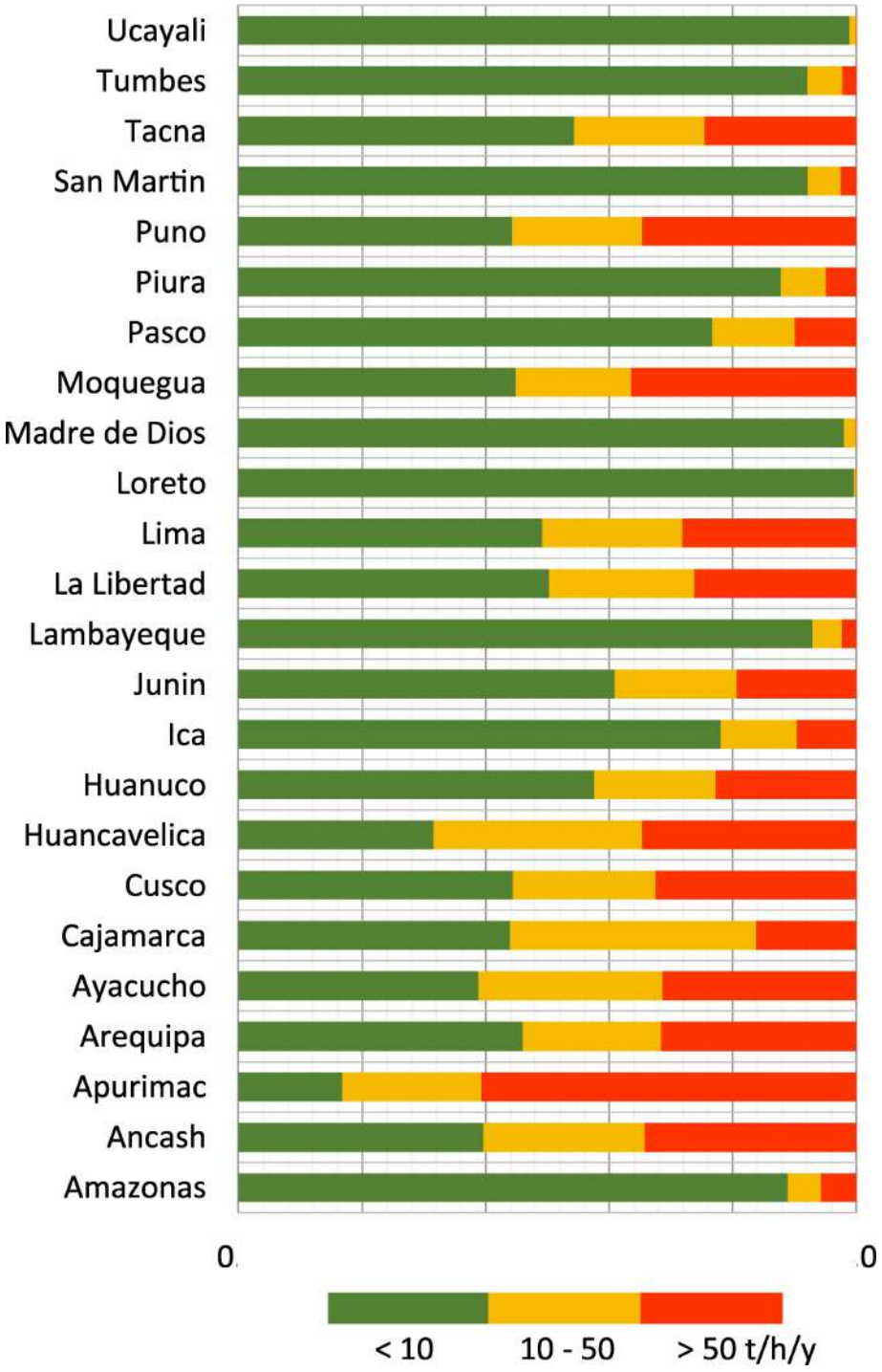
Ucayali
Tumbes
Tacna
San Martin
Puno
Piura
Pasco
Moquegua
Madre de Dios
Loreto
Lima
La Libertad
Lambayeque
Junin
Ica
Huanuco
Huancavelica
Cusco
Cajamarca
Ayacucho
Arequipa
Apurimac
Ancash
Amazonas
0
0
< 10
10 - 50
> 50 t/h/y

Figure 6